

Semileptonic decay $\Lambda_b \rightarrow \Lambda_c + \tau^- + \bar{\nu}_\tau$ in the covariant confined quark model

Thomas Gutsche,¹ Mikhail A. Ivanov,² Jürgen G. Körner,³
Valery E. Lyubovitskij,^{1,4,5} Pietro Santorelli,^{6,7} and Nurgul Habyl⁸

¹ *Institut für Theoretische Physik, Universität Tübingen,*

Kepler Center for Astro and Particle Physics, Auf der Morgenstelle 14, D-72076, Tübingen, Germany

² *Bogoliubov Laboratory of Theoretical Physics, Joint Institute for Nuclear Research, 141980 Dubna, Russia*

³ *PRISMA Cluster of Excellence, Institut für Physik,*

Johannes Gutenberg-Universität, D-55099 Mainz, Germany

⁴ *Department of Physics, Tomsk State University, 634050 Tomsk, Russia*

⁵ *Mathematical Physics Department, Tomsk Polytechnic University, Lenin Avenue 30, 634050 Tomsk, Russia*

⁶ *Dipartimento di Fisica, Università di Napoli Federico II,*

Complesso Universitario di Monte Sant' Angelo, Via Cintia, Edificio 6, 80126 Napoli, Italy

⁷ *Istituto Nazionale di Fisica Nucleare, Sezione di Napoli, 80126 Napoli, Italy*

⁸ *Department of Physics and Technology, Al-Farabi Kazakh National University, 480012 Almaty, Kazakhstan*

Recently there has been much interest in the tauonic semileptonic meson decays $B \rightarrow D + \tau + \nu_\tau$ and $B \rightarrow D^* + \tau + \nu_\tau$, where one has found larger rates than what is predicted by the Standard Model. We analyze the corresponding semileptonic baryon decays $\Lambda_b^0 \rightarrow \Lambda_c^+ + \tau^- + \bar{\nu}_\tau$ with particular emphasis on the lepton helicity flip and scalar contributions which vanish for zero lepton masses. We calculate the total rate, the differential decay distributions, the longitudinal and transverse polarization of the daughter baryon Λ_c^+ and the τ lepton, and the lepton-side forward-backward asymmetries. The nonvanishing polarization of the daughter baryon Λ_c^+ leads to hadron-side asymmetries in e.g. the decay $\Lambda_c^+ \rightarrow \Lambda^0 + \pi^+$ and azimuthal correlations between the two final-state decay planes which we specify. We provide numerical results on these observables using results of the covariant confined quark model. We find large lepton mass effects in the q^2 spectra and in the polarization observables.

PACS numbers: 12.39.Ki, 13.30.Eg, 14.20.Jn, 14.20.Mr

Keywords: relativistic quark model, light and heavy baryons, decay rates and asymmetries

I Introduction

Recently there has been much discussion about tensions and discrepancies in some of the experimental results on leptonic, semileptonic and rare decays involving μ and τ leptons with the predictions of the Standard Model (SM). Among these are the tauonic B decays $\bar{B} \rightarrow \tau \bar{\nu}_\tau$, $\bar{B} \rightarrow D \tau \bar{\nu}_\tau$ and $\bar{B} \rightarrow D^* \tau \bar{\nu}_\tau$ and the muonic decays $B \rightarrow K^* \mu^+ \mu^-$ and $\text{Br}[B \rightarrow K \mu^+ \mu^-]/\text{Br}[B \rightarrow K e^+ e^-]$. The situation has been nicely summarized in Refs. [1–4]. The biggest discrepancies with SM predictions have been reported by the *BaBar* [5] and the Belle collaborations [6, 7] for the decays $B \rightarrow D^{(*)} \tau \bar{\nu}_\tau$. The discrepancy with the SM results has been summarized in Ref. [8] by comparing the SM predictions for the ratios

$$R(\mathcal{D}) \equiv \frac{\text{Br}(\bar{B} \rightarrow \mathcal{D} \tau^- \bar{\nu}_\tau)}{\text{Br}(\bar{B} \rightarrow \mathcal{D} \ell^- \bar{\nu}_\ell)} \quad (\mathcal{D} = D, D^*; \quad \ell = e, \mu) \quad (1)$$

with the experimental results combined from *Babar* and Belle. The SM predictions were found to be smaller than the measurements by almost 3.5 σ :

$$R(D) = \begin{cases} 0.305 \pm 0.012 & \text{SM} \\ 0.421 \pm 0.058 & \text{Babar \& Belle} \end{cases} \quad (2)$$

$$R(D^*) = \begin{cases} 0.252 \pm 0.004 & \text{SM} \\ 0.337 \pm 0.025 & \text{Babar \& Belle.} \end{cases} \quad (3)$$

This observation has inspired a number of searches for new physics beyond the SM (BSM) in charged current interactions. These include the addition of new effective vector, scalar and tensor interactions in addition to the standard $V - A$ interaction. Details can be found in the recent literature on this subject (see, e.g. Refs. [8–21]).

Motivated by the discrepancy between theory and experiment in the meson sector, we analyze the corresponding semileptonic baryon decays $\Lambda_b^0 \rightarrow \Lambda_c^+ + \tau^- + \bar{\nu}_\tau$ within the SM with particular emphasis on the lepton helicity flip contributions which vanish for zero lepton masses. We collect the necessary tools to analyze the semileptonic decay $\Lambda_b^0 \rightarrow \Lambda_c^+ + \ell^- + \bar{\nu}_\ell$ ($\ell = e, \mu, \tau$) as well as the corresponding cascade decay $\Lambda_b^0 \rightarrow \Lambda_c^+(\rightarrow \Lambda^0 + \pi^+) + \ell^- + \bar{\nu}_\ell$. As in Refs. [22–24], we describe the semileptonic decays using the helicity formalism which allows one to include lepton mass and polarization effects without much additional effort.

We calculate the total rate, the differential decay distributions, the longitudinal and transverse polarization of the daughter baryon and lepton-side forward-backward asymmetries. The nonvanishing polarization of the daughter baryon Λ_c^+ leads to hadron-side asymmetries in e.g. the decay $\Lambda_c^+ \rightarrow \Lambda + \pi^+$ and azimuthal correlations between the two final-state decay planes which we specify. We provide numerical results on these observables using results of the covariant confined quark model.

We have split the paper into a model-independent and a model-dependent part. In the first part of the paper, we set up the model-independent helicity analysis leading to compact expressions for angular decay distributions and polarization observables. In the second part, we discuss the dynamics of the current-induced $\Lambda_b \rightarrow \Lambda_c$ transitions in terms of the covariant confined quark model and present our numerical results.

The paper is organized as follows: In Sec. II, we briefly review the helicity formalism for the $\Lambda_b \rightarrow \Lambda_c$ transitions and write down the relations between the helicity and invariant transition amplitudes. In Sec. III, we derive a two-fold angular decay distribution for the three-body decay process $\Lambda_b^0 \rightarrow \Lambda_c^+ + \ell^- + \bar{\nu}_\ell$ ($\ell = e, \mu, \tau$). We define a lepton-side forward-backward asymmetry as well as a convexity parameter which describes the $\cos\theta$ dependence of the angular decay distribution. In Sec. IV, we determine the longitudinal and transverse polarization components of the daughter baryon Λ_c^+ and the charged lepton ℓ^- . In Sec. V, we present the full fourfold angular decay distribution for the cascade decay $\Lambda_b^0 \rightarrow \Lambda_c^+(\rightarrow \Lambda^0 + \pi^+) + \ell^- + \bar{\nu}_\ell$, where we use the narrow-width approximation for the intermediate baryon state Λ_c^+ . In Sec. VI, we present our dynamical input in terms of the covariant confined quark model previously developed by us. We specify the form of the interpolating three-quark currents for the Λ_Q baryons which are needed in our calculation. Our numerical results for the invariant $\Lambda_b \rightarrow \Lambda_c$ transition form factors are presented in terms of simple double-pole rational approximants. In Sec. VII, we present our numerical results for the decay distributions and polarization observables defined in Secs. III–V. Finally, Sec. VIII contains our summary and conclusions. We have collected some technical material in the appendixes. In Appendix A, we use covariant methods to calculate the helicity components of the unpolarized and polarized lepton tensors of the decays $W_{\text{off-shell}}^- \rightarrow \ell^- \bar{\nu}_\ell$ and $W_{\text{off-shell}}^+ \rightarrow \ell^+ \nu_\ell$ including lepton mass effects. In Appendix B, we present results on the helicity amplitudes for the above two leptonic transitions.

II Invariant and helicity amplitudes

The matrix element of the process $\Lambda_b^0(p_1) \rightarrow \Lambda_c^+(p_2) + W_{\text{off-shell}}^-(q)$ is expressed via the vector and axial vector current matrix elements which can be expanded in terms of a complete set of invariants:

$$M_\mu^V(\lambda_1, \lambda_2) = \langle B_2, \lambda_2 | J_\mu^V | B_1, \lambda_1 \rangle = \bar{u}_2(p_2, \lambda_2) \left[F_1^V(q^2) \gamma_\mu - \frac{F_2^V(q^2)}{M_1} i \sigma_{\mu\nu} q^\nu + \frac{F_3^V(q^2)}{M_1} q_\mu \right] u_1(p_1, \lambda_1), \quad (4)$$

$$M_\mu^A(\lambda_1, \lambda_2) = \langle B_2, \lambda_2 | J_\mu^A | B_1, \lambda_1 \rangle = \bar{u}_2(p_2, \lambda_2) \left[F_1^A(q^2) \gamma_\mu - \frac{F_2^A(q^2)}{M_1} i \sigma_{\mu\nu} q^\nu + \frac{F_3^A(q^2)}{M_1} q_\mu \right] \gamma_5 u_1(p_1, \lambda_1) \quad (5)$$

where $\sigma_{\mu\nu} = \frac{i}{2}(\gamma_\mu \gamma_\nu - \gamma_\nu \gamma_\mu)$ and $q = p_1 - p_2$. The labels $\lambda_i = \pm \frac{1}{2}$ denote the helicities of the two baryons. In the present application $B_1 = \Lambda_b$ and $B_2 = \Lambda_c$.

The SM current is not conserved and thus consists of a spin-1 and a spin-0 component where the J^P content of the vector current J_μ^V and the axial vector current J_μ^A are $(0^+, 1^-)$ and $(0^-, 1^+)$, respectively. One defines helicity amplitudes through

$$H_{\lambda_2 \lambda_W}^{V/A} = M_\mu^{V/A}(\lambda_2) \epsilon^{\dagger \mu}(\lambda_W), \quad (6)$$

where there are four helicities for the $W_{\text{off-shell}}^-$, namely $\lambda_W = \pm 1, 0$ ($J = 1$) and $\lambda_W = 0$ ($J = 0$). The label $J = 1, 0$ denotes the two angular momenta of the rest frame $W_{\text{off-shell}}^-$. In order to distinguish the two $\lambda_W = 0$ states we follow the convention of Refs. [23, 24] and adopt the notation $\lambda_W = 0$ for $J = 1$ and $\lambda_W = t$ for $J = 0$ (t for temporal). From angular momentum conservation, one has $\lambda_1 = -\lambda_2 + \lambda_W$.

It is easiest to calculate the helicity amplitudes in the rest frame of the parent baryon B_1 , where we choose the z -axis to be along the $W_{\text{off-shell}}^-$ (see Fig. 1). They read (see e.g. Refs. [25–27])

$$\begin{aligned} H_{+\frac{1}{2}t}^{V/A} &= \frac{\sqrt{Q_\pm}}{\sqrt{q^2}} \left(M_\mp F_1^{V/A} \pm \frac{q^2}{M_1} F_3^{V/A} \right), \\ H_{+\frac{1}{2}+1}^{V/A} &= \sqrt{2Q_\mp} \left(F_1^{V/A} \pm \frac{M_\pm}{M_1} F_2^{V/A} \right), \\ H_{+\frac{1}{2}0}^{V/A} &= \frac{\sqrt{Q_\mp}}{\sqrt{q^2}} \left(M_\pm F_1^{V/A} \pm \frac{q^2}{M_1} F_2^{V/A} \right). \end{aligned} \quad (7)$$

where we make use of the abbreviations $M_\pm = M_1 \pm M_2$ and $Q_\pm = M_\pm^2 - q^2$.

From parity or from an explicit calculation, one has

$$H_{-\lambda_2, -\lambda_W}^V = H_{\lambda_2, \lambda_W}^V, \quad H_{-\lambda_2, -\lambda_W}^A = -H_{\lambda_2, \lambda_W}^A. \quad (8)$$

The total left-chiral helicity amplitude is defined by the composition

$$H_{\lambda_2, \lambda_W} = H_{\lambda_2, \lambda_W}^V - H_{\lambda_2, \lambda_W}^A. \quad (9)$$

The polarization observables to be discussed further on can be expressed in terms of helicity structure functions given in terms of bilinear combinations of helicity amplitudes. The definitions of the structure functions are collected in Table I. Eleven of these contribute to the partial rates and polarization observables discussed in this paper. For the sake of completeness, we have also listed the structure function \mathcal{H}_{ST} , which enters in the description of polarized Λ_b decay which we, however, do not discuss in this paper.

The helicity structure functions have definite parity properties as indicated in Table I. The first and second columns of Table I list the parity-conserving (p.c.) and parity-violating (p.v.) bilinear combinations of helicity amplitudes, respectively; i.e., the p.c. and p.v. helicity structure functions result from products of VV and AA , and VA and AV currents, respectively.

The vector and axial vector helicity amplitudes possess simple structures in the kinematical limits of zero and maximal recoil. At the zero recoil point $q^2 \rightarrow (M_1 - M_2)^2$, one has only s -wave transitions (conventionally called allowed Fermi and allowed Gamow-Teller transitions, respectively). The surviving helicity amplitudes are

$$H_{\frac{1}{2}t}^V = H_{-\frac{1}{2}t}^V = 2\sqrt{M_1 M_2} \left(F_1^V + \frac{M_-}{M_1} F_3^V \right) \quad \text{allowed Fermi}, \quad (10)$$

$$H_{\frac{1}{2}1}^A / \sqrt{2} = H_{\frac{1}{2}0}^A = 2\sqrt{M_1 M_2} \left(F_1^A - \frac{M_-}{M_1} F_2^A \right) \quad \text{allowed Gamow - Teller}. \quad (11)$$

TABLE I: Definition of helicity structure functions and their parity properties.

Parity-conserving (p.c.)	parity-violating (p.v.)
$\mathcal{H}_U = H_{+\frac{1}{2}+1} ^2 + H_{-\frac{1}{2}-1} ^2$	$\mathcal{H}_P = H_{+\frac{1}{2}+1} ^2 - H_{-\frac{1}{2}-1} ^2$
$\mathcal{H}_L = H_{+\frac{1}{2}0} ^2 + H_{-\frac{1}{2}0} ^2$	$\mathcal{H}_{LP} = H_{+\frac{1}{2}0} ^2 - H_{-\frac{1}{2}0} ^2$
$\mathcal{H}_S = H_{+\frac{1}{2}t} ^2 + H_{-\frac{1}{2}t} ^2$	$\mathcal{H}_{SP} = H_{+\frac{1}{2}t} ^2 - H_{-\frac{1}{2}t} ^2$
$\mathcal{H}_{LT} = \text{Re} \left(H_{+\frac{1}{2}+1} H_{-\frac{1}{2}0}^\dagger + H_{+\frac{1}{2}0} H_{-\frac{1}{2}-1}^\dagger \right)$	$\mathcal{H}_{LTP} = \text{Re} \left(H_{+\frac{1}{2}+1} H_{-\frac{1}{2}0}^\dagger - H_{+\frac{1}{2}0} H_{-\frac{1}{2}-1}^\dagger \right)$
$\mathcal{H}_{ST} = \text{Re} \left(H_{+\frac{1}{2}+1} H_{-\frac{1}{2}t}^\dagger + H_{+\frac{1}{2}t} H_{-\frac{1}{2}-1}^\dagger \right)$	$\mathcal{H}_{STP} = \text{Re} \left(H_{+\frac{1}{2}+1} H_{-\frac{1}{2}t}^\dagger - H_{+\frac{1}{2}t} H_{-\frac{1}{2}-1}^\dagger \right)$
$\mathcal{H}_{SL} = \text{Re} \left(H_{+\frac{1}{2}0} H_{+\frac{1}{2}t}^\dagger + H_{-\frac{1}{2}0} H_{-\frac{1}{2}t}^\dagger \right)$	$\mathcal{H}_{SLP} = \text{Re} \left(H_{+\frac{1}{2}0} H_{+\frac{1}{2}t}^\dagger - H_{-\frac{1}{2}0} H_{-\frac{1}{2}t}^\dagger \right)$

The zero recoil structure has implications for the structure functions. At zero recoil, one finds

$$\mathcal{H}_{ST}, \mathcal{H}_{SL}, \mathcal{H}_P, \mathcal{H}_{LP}, \mathcal{H}_{SP}, \mathcal{H}_{LTP} = 0, \quad \mathcal{H}_U = 2\mathcal{H}_L = \sqrt{2}\mathcal{H}_{LT}. \quad (12)$$

At $q^2 = 0$ (which is very close to the maximal recoil point for the e and μ modes), the scalar and longitudinal helicity amplitudes dominate. At $q^2 = 0$ one has

$$H_{\pm\frac{1}{2}t} = H_{\pm\frac{1}{2}0} \sim (F_1^V \mp F_1^A). \quad (13)$$

As we shall see later on, the results of our dynamical quark model are quite close to the heavy quark effective theory HQET result $F_1^V(q^2) = F_1^A(q^2) = F(q^2)$, $F_{2,3}^{V/A} = 0$ (see e.g. the review in Ref. [28]). It is therefore quite useful to list the HQET relations for the helicity amplitudes and structure functions. In the HQET limit, one has

$$H_{\frac{1}{2}0} = -H_{\frac{1}{2}t}, \quad H_{-\frac{1}{2}0} = H_{-\frac{1}{2}t}, \quad (14)$$

which leads to the structure function relations

$$\mathcal{H}_{SP} = \mathcal{H}_{LP} = -\mathcal{H}_{SL}, \quad \mathcal{H}_L = \mathcal{H}_S = -\mathcal{H}_{SLP}, \quad \mathcal{H}_{ST} = \mathcal{H}_{LTP}, \quad \mathcal{H}_{STP} = \mathcal{H}_{LT}. \quad (15)$$

If one combines the zero recoil structure with the HQET results, one finds the zero recoil amplitude relations

$$H_{\frac{1}{2}t} = H_{\frac{1}{2}0} = H_{\frac{1}{2}1}/\sqrt{2} = H_{-\frac{1}{2}t} = -H_{\frac{1}{2}0} = -H_{-\frac{1}{2}-1}/\sqrt{2}. \quad (16)$$

At maximal recoil for the (e, μ) modes the HQET relations (13) turn into the helicity amplitude relations

$$H_{\frac{1}{2}t} = H_{\frac{1}{2}0} = 0, \quad H_{-\frac{1}{2}t} = H_{-\frac{1}{2}0}. \quad (17)$$

We have gone to great lengths to describe the limiting values of the structure functions at both ends of the kinematical q^2 range. These limiting values allow us to understand most of the the limiting behavior of our numerical results on the polarization observables at zero recoil and maximal recoil to be discussed in Sec. VII. Similar limiting relations have been discussed before in Ref. [29] for the zero lepton mass case.

The helicity amplitudes H_{λ_2, λ_W} are a superposition of vector and axial vector pieces and thus do not have definite parity properties. One can project back to the vector and axial vector helicity amplitudes by defining the transversity amplitudes [30]:

$$\begin{aligned} A_{\lambda_2\parallel/\perp} &= (H_{\lambda_2+1}^{V-A} \pm H_{-\lambda_2-1}^{V-A})/\sqrt{2}, \\ A_{\lambda_20}^{V/A} &= (H_{\lambda_20}^{V-A} \pm H_{-\lambda_20}^{V-A})/\sqrt{2}, \\ A_{\lambda_2t}^{V/A} &= (H_{\lambda_2t}^{V-A} \pm H_{-\lambda_2t}^{V-A})/\sqrt{2}. \end{aligned} \quad (18)$$

From Eq. (18), one can see that the transversity amplitudes have definite transformation properties under parity, e.g. $A_{\lambda_2\parallel} = A_{-\lambda_2\parallel}$, $A_{\lambda_2\perp} = -A_{-\lambda_2\perp}$, etc.

For the structure functions in Table I, one obtains e.g.

$$\mathcal{H}_U = |A_{\lambda_{2\parallel}}|^2 + |A_{\lambda_{2\perp}}|^2, \quad \mathcal{H}_P = 2 \operatorname{Re} (A_{\lambda_{2\parallel}} A_{\lambda_{2\perp}}^\dagger). \quad (19)$$

The transversity amplitudes correspond to the Cartesian components of the helicity amplitudes. The parity properties of the various structure functions in the transversity representation are clearly manifest. They are identical to those in the helicity representation where they are not quite manifest.

III Twofold angular decay distribution

We first consider the three-particle decay $\Lambda_b^0(p_1) \rightarrow \Lambda_c^+(p_2) + W_{\text{off-shell}}^- \left(\rightarrow \ell^-(p_\ell) + \bar{\nu}_\ell(p_{\nu_\ell}) \right)$ with $q = p_\ell + p_{\nu_\ell}$, $p_\ell^2 = m_\ell^2$, and $p_{\nu_\ell}^2 = 0$. At the present stage we sum over the helicities of the parent and daughter baryon. The three-body decay can be described in terms of the invariant variable q^2 and the polar angle θ defined in Fig. 1. The differential $(q^2, \cos\theta)$ distribution reads

$$\frac{d\Gamma}{dq^2 d\cos\theta} = \frac{G_F^2}{(2\pi)^4} |V_{bc}|^2 \frac{(q^2 - m_\ell^2) |\mathbf{p}_2|}{128 M_1^2 q^2} H^{\mu\nu} L_{\mu\nu}(\theta) \quad (20)$$

where $|\mathbf{p}_2| = \lambda^{1/2}(M_1^2, M_2^2, q^2)/(2M_1) = \sqrt{Q_+ Q_-}/(2M_1)$ is the momentum of the daughter baryon in the Λ_b rest frame. The lepton tensor $L_{\mu\nu}$ can be calculated as (see Appendix A)

$$L^{\mu\nu} = 8 \left(p_\ell^\mu p_{\nu_\ell}^\nu + p_\ell^\nu p_{\nu_\ell}^\mu - \frac{1}{2}(q^2 - m_\ell^2) g^{\mu\nu} + i \varepsilon^{\mu\nu\alpha\beta} p_{\ell\alpha} p_{\nu_\ell\beta} \right), \quad (21)$$

where $\varepsilon_{0123} = +1$. The hadron tensor $H_{\mu\nu}$ is given by the tensor product of the chiral matrix elements

$$H_{\mu\nu} = M_\mu M_\nu^\dagger, \quad M_\mu = M_\mu^V - M_\mu^A, \quad (22)$$

where the vector and axial vector matrix elements are defined in Eq. (4).

The $\cos\theta$ dependence of $H_{\mu\nu} L^{\mu\nu}(\theta)$ can be worked out by following the methods described in Ref. [22–24] and later on adopted by Fajfer *et al.* [15] in their analysis of BSM effects in the decays $\bar{B} \rightarrow D^{(*)} \tau \bar{\nu}_\tau$. Note that the $\cos\theta$ dependence can also be worked out by using traditional methods by a straightforward contraction of $H_{\mu\nu} L^{\mu\nu}(\theta)$. This leads to expressions involving scalar products of momenta that are defined in different reference frames. When doing the required contractions, the four-momenta have to be boosted to a common reference frame as e.g. described in Ref. [31] for the decay $H \rightarrow Z^0 \ell^+ \ell^-$ and in Ref. [32] for the decay $K^\pm \rightarrow \pi^\pm \pi^0 e^+ e^-$. The advantage of the helicity method is that the origin of the angular factors multiplying the helicity structure functions can be straightforwardly identified. One makes use of the completeness relation for the polarization four-vectors

$$\sum_{m, m' = t, \pm, 0} \epsilon^\mu(m) \epsilon^{\dagger\nu}(m') g_{mm'} = g^{\mu\nu}. \quad (23)$$

The tensor $g_{mm'} = \text{diag}(+, -, -, -)$ is the spherical representation of the metric tensor, where the components are ordered in the sequence $m, m' = t, +, 0, -$.

Using the completeness relation (23), one can rewrite the contraction of the hadron and lepton tensors $H_{\mu\nu} L^{\mu\nu}(\theta)$ as a sum over products of their respective helicity components. Appropriate to the problem, we replace the labels (m, m') with the helicity components (λ_W, λ'_W) of the $W_{\text{off-shell}}^-$. One finds

$$\begin{aligned} H_{\mu\nu} L^{\mu\nu}(\theta) &= H^{\mu'\nu'} g_{\mu'\mu} g_{\nu'\nu} L^{\mu\nu}(\theta) \\ &= \sum_{\lambda_W, \lambda'_W, \lambda''_W, \lambda'''_W} H^{\mu'\nu'} \epsilon_{\mu'}(\lambda_W) \epsilon_{\mu'}^\dagger(\lambda'_W) g_{\lambda_W \lambda'_W} \epsilon_{\nu'}(\lambda''_W) \epsilon_{\nu'}^\dagger(\lambda'''_W) g_{\lambda''_W \lambda'''_W} L^{\mu\nu}(\theta) \\ &= \sum_{\lambda_W, \lambda'_W, \lambda''_W, \lambda'''_W} \left(H^{\mu'\nu'} \epsilon_{\mu'}(\lambda_W) \epsilon_{\nu'}^\dagger(\lambda'_W) \right) \left(L^{\mu\nu}(\theta) \epsilon_{\mu'}^\dagger(\lambda'_W) \epsilon_{\nu'}(\lambda''_W) \right) g_{\lambda_W \lambda'_W} g_{\lambda''_W \lambda'''_W} \\ &\equiv \sum_{\lambda_W \lambda'_W} H_{\lambda_W \lambda'_W} L_{\lambda_W \lambda'_W}(\theta) g_{\lambda_W \lambda'_W} g_{\lambda'_W \lambda'_W}. \end{aligned} \quad (24)$$

The two factors enclosed by round brackets in the third line of Eq.(24) are Lorentz invariant and can thus be evaluated in different Lorentz frames. The leptonic part will be evaluated in the (ℓ, ν_ℓ) CM frame (or $W_{\text{off-shell}}$ rest frame) with the positive z axis along the $W_{\text{off-shell}}$ bringing in the decay angle θ . The hadronic part is evaluated in the Λ_b rest frame bringing in the helicity amplitudes [Eq. (7)].

The product of the two spherical metric tensors $g_{\lambda_W \lambda_W} g_{\lambda'_W \lambda'_W}$ in the last line of (24) gives +1 for $\lambda_W = t, \lambda'_W = t$ and $\lambda_W = i, \lambda'_W = j$ ($i, j = 1, 0, -1$) and -1 for $\lambda_W = t, \lambda'_W = i$ ($i = 1, 0, -1$) and $\lambda_W = i, \lambda'_W = t$ ($i = 1, 0, -1$); i.e., there is an extra minus sign for the spin 0–spin 1 interference contribution. We can therefore rewrite the last line of Eq. (24) as

$$H_{\mu\nu} L^{\mu\nu}(\theta) = \sum_{\lambda_W, \lambda'_W} (-1)^{J+J'} H_{\lambda_W \lambda'_W} L_{\lambda_W \lambda'_W}(\theta), \quad (25)$$

where the sum is over $\lambda_W, \lambda'_W = t, \pm 1, 0$. Note that, through the choice of the “t” notation, the dependence of $H_{\lambda_W \lambda'_W}$ and $L_{\lambda_W \lambda'_W}(\theta)$ on J, J' is implicit.

Referring to the factorized form Eq. (22), the helicity representation of the hadron tensor can also be written in terms of bilinear products of the helicity amplitudes, i.e.

$$\mathcal{H}_{\lambda_W \lambda'_W} = \sum_{\lambda_2} H_{\lambda_2 \lambda_W} H_{\lambda_2 \lambda'_W}^\dagger, \quad (26)$$

where the three helicities of the process satisfy the angular momentum constraint $\lambda_1 = \lambda_2 - \lambda_W$.

One has to remember that Eq. (20) refers to the differential decay rate of an unpolarized parent baryon into a daughter baryon whose spin is not observed. Together with the angular momentum constraint $\lambda_1 = \lambda_2 - \lambda_W$, this implies $\lambda_W = \lambda'_W$. One therefore has diagonal contributions $\lambda_W = \lambda'_W = t, \pm 1, 0$ as well as quasi-diagonal contributions with $\lambda_W = t$ and $\lambda'_W = 0$ and vice versa.

Using the factorized form (26), Eq. (25) turns into

$$H_{\mu\nu} L^{\mu\nu}(\theta) = \sum_{\lambda_W, \lambda'_W, \lambda_2} (-1)^{J+J'} \delta_{\lambda_2 - \lambda_W, \lambda_2 - \lambda'_W} H_{\lambda_2 \lambda_W} H_{\lambda_2 \lambda'_W}^\dagger L_{\lambda_W \lambda'_W}(\theta), \quad (27)$$

where the delta function $\delta_{\lambda_2 - \lambda_W, \lambda_2 - \lambda'_W}$ encodes the fact mentioned above that we are dealing with the decay of an unpolarized parent baryon B_1 into a daughter baryon B_2 whose spin is not observed. The helicity components of the lepton tensor $L_{\lambda_W \lambda'_W}(\theta)$ have been calculated in Appendix A [see Eq. (A6)].

One can go one step further and express the leptonic helicity tensor $L_{\lambda_W \lambda'_W}(\theta)$ in terms of the leptonic helicity amplitudes $h_{\lambda_\ell \lambda_{\bar{\nu}_\ell} = 1/2}(J)$ defined in Appendix B. They describe the decay $W_{\text{off-shell}}^- \rightarrow \ell^- \bar{\nu}_\ell$, where the z -direction is along the charged lepton ℓ^- . We shall refer to this frame as the W -decay frame. Then one has to rotate the leptonic helicity amplitudes defined in the W -decay frame to the original z -direction employing Wigner's $d_{mm'}^J(\theta)$ functions (as in Ref. [33] we use the convention of Rose [34] for the d -functions). One then has ($d_{00}^0 = 1$)

$$L_{\lambda_W \lambda'_W}(\theta) = \sum_{\lambda_\ell} d_{\lambda_W, \lambda_\ell - 1/2}^J(\theta) d_{\lambda'_W, \lambda_\ell - 1/2}^{J'}(\theta) h_{\lambda_\ell 1/2}(J) h_{\lambda_\ell 1/2}^\dagger(J'). \quad (28)$$

The leptonic helicity amplitudes $h_{\lambda_\ell - 1/2}(J)$ have been calculated in Appendix B. We mention that the representation (28) has been used to check the results of the covariant determination of $L_{\lambda_W \lambda'_W}(\theta)$ used in (27).

Returning to the representation in Eq. (27), one finds using the results of Appendix A ($v = 1 - m_\ell^2/q^2$)

$$H_{\mu\nu} L^{\mu\nu}(\theta) = \frac{16\pi}{3} (2q^2 v) W(\theta), \quad (29)$$

with

$$W(\theta) = \frac{3}{8} (1 + \cos^2 \theta) \mathcal{H}_U - \frac{3}{4} \cos \theta \mathcal{H}_P + \frac{3}{4} \sin^2 \theta \mathcal{H}_L + \delta_\ell \left\{ \frac{3}{2} \mathcal{H}_S + \frac{3}{4} \sin^2 \theta \mathcal{H}_U + \frac{3}{2} \cos^2 \theta \mathcal{H}_L - 3 \cos \theta \mathcal{H}_{SL} \right\}. \quad (30)$$

The first three terms in (30) result from lepton helicity nonflip (nf) contributions, while the last four terms proportional to δ_ℓ are lepton helicity flip (hf) contributions, where the helicity flip suppression factor is given by (see Appendix B)

$$\delta_\ell = \frac{m_\ell^2}{2q^2}. \quad (31)$$

It is interesting to note that of the two observables \mathcal{H}_P and \mathcal{H}_{SL} that multiply the parity-odd angular factor $\cos\theta$ in Eq. (30), \mathcal{H}_P is parity violating whereas \mathcal{H}_{SL} is parity conserving (see Table I). In the latter case, the parity-odd nature results from the parity-even but parity-odd interference of the $(0^+, 1^-)$ pieces in the (VV) term and the $(0^-, 1^+)$ pieces in the (AA) term.

Integrating over $\cos\theta$ and putting in the correct normalization, one obtains the normalized differential rate, which reads

$$\frac{d\Gamma}{dq^2} = \Gamma_0 \frac{(q^2 - m_\ell^2)^2 |\mathbf{p}_2|}{M_1^7 q^2} \left\{ \mathcal{H}_U + \mathcal{H}_L + \delta_\ell [\mathcal{H}_U + \mathcal{H}_L + 3\mathcal{H}_S] \right\} \equiv \Gamma_0 \frac{(q^2 - m_\ell^2)^2 |\mathbf{p}_2|}{M_1^7 q^2} \mathcal{H}_{\text{tot}}, \quad (32)$$

where

$$\mathcal{H}_{\text{tot}} = \int d\cos\theta W(\theta) = \mathcal{H}_U + \mathcal{H}_L + \delta_\ell [\mathcal{H}_U + \mathcal{H}_L + 3\mathcal{H}_S]. \quad (33)$$

In (32), we have introduced the Born term rate

$$\Gamma_0 = \frac{G_F^2 |V_{bc}|^2 M_1^5}{192\pi^3}. \quad (34)$$

The rate Γ_0 represents the SM rate of the decay of a massive parent fermion into three massless fermions, i.e. $M_1 \neq 0$ and $M_2, m_\ell, m_{\nu_\ell} = 0$, where $F_1^{V/A} = 1$ and $F_{2,3}^{V/A} = 0$. The q^2 -dependent factor multiplying Γ_0 in Eq.(32) can be seen to be integrated to 1 for these mass and form factor settings.

It is convenient to define partial rates $d\Gamma_X/dq^2$ and $d\tilde{\Gamma}_X/dq^2$ for the helicity nonflip (nf) and helicity flip (hf) helicity structure functions \mathcal{H}_X defined in Table I. $d\Gamma_X/dq^2$ refers to a lepton helicity nonflip (*nf*) rate, while $d\tilde{\Gamma}_X/dq^2$ refers to a lepton helicity flip (*hf*) rate. One has

$$\begin{aligned} \frac{d\Gamma_X}{dq^2}(nf) &= \Gamma_0 \frac{(q^2 - m_\ell^2)^2 |\mathbf{p}_2|}{M_1^7 q^2} \mathcal{H}_X, & X = U, L, P, L_P, LT, LTP, \\ \frac{d\tilde{\Gamma}_X}{dq^2}(hf) &= \delta_\ell \Gamma_0 \frac{(q^2 - m_\ell^2)^2 |\mathbf{p}_2|}{M_1^7 q^2} \mathcal{H}_X, & X = U, L, LT, P, SL, S, L_P, S_P, SL_P, LTP, STP. \end{aligned} \quad (35)$$

The partial rates can then be split into a helicity nonflip (*nf*) and helicity flip (*hf*) part according to

$$\frac{d\Gamma_X}{dq^2} = \frac{d\Gamma_X}{dq^2}(nf) + \frac{d\tilde{\Gamma}_X}{dq^2}(hf). \quad (36)$$

It is clear that the (un-normalized) longitudinal polarization of the charged lepton for a given helicity structure function \mathcal{H}_X is then given by

$$P_z^\ell(X) \sim d\tilde{\Gamma}_X/dq^2 - d\Gamma_X/dq^2 \quad (37)$$

The distribution Eq. (30) is given in terms of a second-order polynomial in $\cos\theta$. The linear term results in a forward-backward asymmetry defined by

$$A_{FB}^\ell(q^2) = \frac{d\Gamma(F) - d\Gamma(B)}{d\Gamma(F) + d\Gamma(B)} = -\frac{3\mathcal{H}_P + 4\delta_\ell \mathcal{H}_{SL}}{2\mathcal{H}_{\text{tot}}}. \quad (38)$$

The quadratic term can be isolated by taking the second derivative of (30). We therefore define a convexity parameter $C_F(q^2)$ according to

$$C_F(q^2) = \frac{1}{\mathcal{H}_{\text{tot}}} \frac{d^2 W(\theta)}{d(\cos\theta)^2} = \frac{3}{4} (1 - 2\delta_\ell) \frac{\mathcal{H}_U - 2\mathcal{H}_L}{\mathcal{H}_{\text{tot}}}. \quad (39)$$

IV Polarization of the daughter baryon Λ_c and the charged lepton ℓ^-

The polarization components of the daughter baryon B_2 ($B_2 = \Lambda_c$ in the present application) can be obtained from the spin density matrix of the daughter baryon. In Eq. (27) we have taken the sum over helicities of the daughter

baryon B_2 or, put in a different language, we have taken the trace of the polarization density matrix $\rho_{\lambda_2 \lambda'_2}$ of the daughter baryon B_2 . In order to calculate the polarization components of the daughter baryon, we need to consider the polarization density matrix components $(\rho_{1/2 1/2} - \rho_{-1/2 -1/2})$ for P_z and $2\text{Re}\rho_{1/2 -1/2}$ for P_x ; i.e., we have to allow for $\lambda_2 \neq \lambda'_2$ in Eq. (27). According to Eq. (27) the un-normalized density matrix components of the daughter baryon B_2 read

$$\rho_{\lambda_2 \lambda'_2} = \sum_{\lambda_W, \lambda'_W} (-1)^{J+J'} \delta_{\lambda_2 - \lambda_W, \lambda'_2 - \lambda'_W} H_{\lambda_2 \lambda_W} H_{\lambda'_2 \lambda'_W}^\dagger L_{\lambda_W \lambda'_W}(\theta), \quad (40)$$

The polarization can be seen to be $\cos\theta$ dependent. Instead of considering the full θ -dependent polarization components we take the mean of $P_x(\theta)$ and $P_z(\theta)$ with regard to $\cos\theta$. One obtains

$$\begin{aligned} P_z^h(q^2) &= \frac{\rho_{1/2 1/2} - \rho_{-1/2 -1/2}}{\rho_{1/2 1/2} + \rho_{-1/2 -1/2}} = \frac{\mathcal{H}_P + \mathcal{H}_{LP} + \delta_\ell(\mathcal{H}_P + \mathcal{H}_{LP} + 3\mathcal{H}_{SP})}{\mathcal{H}_{\text{tot}}}, \\ P_x^h(q^2) &= \frac{2\text{Re}\rho_{1/2 -1/2}}{\rho_{1/2 1/2} + \rho_{-1/2 -1/2}} = -\frac{3\pi}{4\sqrt{2}} \frac{\mathcal{H}_{LT} - 2\delta_\ell \mathcal{H}_{STP}}{\mathcal{H}_{\text{tot}}}. \end{aligned} \quad (41)$$

The corresponding θ -dependent expressions are written down in Sec. IV.

In the zero lepton mass limit, the charged lepton ℓ^- is 100% polarized opposite to its momentum direction (i.e. it has negative helicity). Lepton mass effects bring in helicity flip contributions which can considerably change the magnitude of the polarization $|\vec{P}^\ell|$ and its orientation. In Appendix A we have calculated the lepton's polarization components $P_x^\ell(\theta)$ and $P_z^\ell(\theta)$. Again, we consider only the $\cos\theta$ averaged polarization. Using the results of Appendix A, one finds

$$\begin{aligned} P_z^\ell(q^2) &= -\frac{\mathcal{H}_U + \mathcal{H}_L - \delta_\ell(\mathcal{H}_U + \mathcal{H}_L + 3\mathcal{H}_S)}{\mathcal{H}_{\text{tot}}}, \\ P_x^\ell(q^2) &= -\frac{3\pi}{4\sqrt{2}} \sqrt{\delta_\ell} \frac{\mathcal{H}_P - 2\mathcal{H}_{SL}}{\mathcal{H}_{\text{tot}}}. \end{aligned} \quad (42)$$

The corresponding θ dependent components can be obtained from Appendix A. The longitudinal polarization $P_z^\ell(q^2)$ can be seen to have the rate structure $(\Gamma(hf) - \Gamma(nf))/(\Gamma(hf) + \Gamma(nf))$ in agreement with Eq. (42). Note that the scalar-longitudinal piece \mathcal{H}_{SL} in (42) contains an extra minus sign resulting from the factor $(-1)^{J+J'}$.

When calculating the q^2 averages of the components of \vec{P}^h and \vec{P}^ℓ , one has to reinstate the common q^2 -dependent factor $(q^2 - m_\ell^2)^2 |\mathbf{p}_2|/q^2$ in the numerator and denominator of the right-hand sides of Eqs. (41) and (42).

V Fourfold angular decay distribution

In the previous section, we have calculated the polarization of the charmed baryon Λ_c^+ in the three-body decay $\Lambda_b^0 \rightarrow \Lambda_c^+ + \ell^- \bar{\nu}_\ell$. The polarization of the Λ_c^+ can be probed by analyzing the angular decay distribution of the subsequent decay of the Λ_c^+ . As an exemplary case we shall consider the decay mode $\Lambda_c^+ \rightarrow \Lambda^0 + \pi^+$ as polarization analyzer. We shall discuss some other important decay modes of the Λ_c^+ at the end of this section.

One can exploit the cascade nature of the decay $\Lambda_b^0 \rightarrow \Lambda_c^+ (\rightarrow \Lambda^0 + \pi^+) + W_{\text{off-shell}}^- (\rightarrow \ell^- + \bar{\nu}_\ell)$ by writing down a joint angular decay distribution involving the polar angles θ, θ_B and the azimuthal angles χ defined by the decay products in their respective CM (center of mass) systems as shown in Fig. 1. The angular decay distribution involves the helicity amplitudes $H_{\lambda_{\Lambda_c} \lambda_W}$ for the decay $\Lambda_b \rightarrow \Lambda_c + W$ and $h_{\lambda_{\Lambda^0}}^B$ for the decay $\Lambda_c^+ \rightarrow \Lambda^0 + \pi^+$. The joint angular decay distribution for the decay of an unpolarized Λ_b reads

$$\begin{aligned} W(\theta, \theta_B, \chi) &= \sum_{\lambda_W, \lambda'_W, \lambda_2, \lambda'_2, \lambda_3} (-1)^{J+J'} d_{\lambda_2 \lambda_3}^{1/2}(\theta_B) d_{\lambda'_2 \lambda_3}^{1/2}(\theta_B) h_{\lambda_3 0}^B h_{\lambda_3 0}^{B\dagger} \\ &\times \delta_{\lambda_W - \lambda_2, \lambda'_W - \lambda'_2} H_{\lambda_2 \lambda_W} H_{\lambda'_2 \lambda'_W}^\dagger L_{\lambda_W \lambda'_W}(\theta, \chi) \end{aligned} \quad (43)$$

where the θ - and χ -dependent leptonic helicity tensor $L_{\lambda_W \lambda'_W}(\theta, \chi)$ is given in Appendix A.

For computer processing, we have taken a slight variant of (43) where we drop the " $\lambda_W = t$ " convention and make up for this by introducing an explicit (J, J') dependence for the hadronic and leptonic helicity amplitudes. Also, we

express the leptonic helicity tensor $L_{\lambda_W \lambda'_W}(\theta, \chi)$ in terms of rotated products of leptonic helicity similar to (28) but now including also the azimuthal rotation. One has

$$L_{\lambda_W \lambda'_W}(\theta, \chi) = d_{\lambda_W, \lambda_\ell - 1/2}^J(\theta) d_{\lambda'_W, \lambda_\ell - 1/2}^{J'}(\theta) e^{i(\lambda_W - \lambda'_W)\chi} h_{\lambda_\ell, \lambda_{\bar{\nu}_\ell = 1/2}}(J) h_{\lambda_\ell, \lambda_{\bar{\nu}_\ell = 1/2}}(J'). \quad (44)$$

Our master formula for the general angular decay distribution then reads

$$\begin{aligned} W(\theta, \theta_B, \chi) &= \sum_{\text{set}} (-1)^{J+J'} d_{\lambda_2 \lambda_3}^{1/2}(\theta_B) d_{\lambda'_2 \lambda_3}^{1/2}(\theta_B) h_{\lambda_3 0}^B h_{\lambda_3 0}^{B\dagger} \\ &\times (\delta_{\lambda_W - \lambda_2, +1/2} + \delta_{\lambda_W - \lambda_2, -1/2}) \delta_{\lambda_W - \lambda_2, \lambda'_W - \lambda'_2} H_{\lambda_2 \lambda_W}(J) H_{\lambda'_2 \lambda'_W}^\dagger(J') \\ &\times d_{\lambda_W, \lambda_\ell - 1/2}^J(\theta) d_{\lambda'_W, \lambda_\ell - 1/2}^{J'}(\theta) e^{i(\lambda_W - \lambda'_W)\chi} h_{\lambda_\ell, \lambda_{\bar{\nu}_\ell = 1/2}}(J) h_{\lambda_\ell, \lambda_{\bar{\nu}_\ell = 1/2}}(J'). \end{aligned} \quad (45)$$

The summation is performed over the following set of the indices:

$$\text{set} = \left\{ \lambda_\ell, \lambda_2, \lambda'_2, \lambda_3 = \pm \frac{1}{2}, \quad \lambda_W, \lambda'_W = \pm 1, 0, \quad J, J' = 0, 1 \right\}, \quad (46)$$

where, in the present application, $B_1 = \Lambda_b$, $B_2 = \Lambda_c$ and $B_3 = \Lambda$. Note that the set (46) does not contain a summation over $\lambda_W = t$ because this is now replaced by the sum over J, J' . As before, the Kronecker symbol $\delta_{\lambda_W - \lambda_2, \lambda'_W - \lambda'_2}$ in Eq. (43) expresses the fact that we are considering the decay of an unpolarized Λ_b . We have also introduced a second Kronecker symbol in Eq. (43), which expresses the fact that the parent baryon is a spin-1/2 particle, implying $|\lambda_W - \lambda_2| = |\lambda'_W - \lambda'_2| = 1/2$. The latter condition is expressed through the Kronecker symbol $(\delta_{\lambda_W - \lambda_2, +1/2} + \delta_{\lambda_W - \lambda_2, -1/2})$. The $d_{mm'}^j$ with $(j = 0, 1/2, 1)$ are Wigner's d -functions, where $d_{00}^0 = 1$. We mention that it is not difficult to generalize Eq. (43) to the case of a decaying polarized Λ_b , as has been done in corresponding baryonic cascade decay calculations in Refs. [26, 33, 35–38].

After factoring out the $\Lambda_c^+ \rightarrow \Lambda^0 + \pi^+$ rate term $(|h_{+\frac{1}{2}0}^B|^2 + |h_{-\frac{1}{2}0}^B|^2)$, one obtains

$$\begin{aligned} W(\theta, \theta_B, \chi) &= \frac{8q^2 v}{3} \left(|h_{+\frac{1}{2}0}^B|^2 + |h_{-\frac{1}{2}0}^B|^2 \right) \left\{ \frac{3}{8} (1 + \cos^2 \theta) \mathcal{H}_U \mp \frac{3}{4} \cos \theta \mathcal{H}_P + \frac{3}{4} \sin^2 \theta \mathcal{H}_L \right. \\ &+ \delta_\ell \left(\frac{3}{4} \sin^2 \theta \mathcal{H}_U + \frac{3}{2} \cos^2 \theta \mathcal{H}_L - 3 \cos \theta \mathcal{H}_{SL} + \frac{3}{2} \mathcal{H}_S \right) \\ &+ \alpha_B \cos \theta_B \left[\frac{3}{8} (1 + \cos^2 \theta) \mathcal{H}_P \mp \frac{3}{4} \cos \theta \mathcal{H}_U + \frac{3}{4} \sin^2 \theta \mathcal{H}_{LP} \right. \\ &+ \delta_\ell \left(\frac{3}{2} \cos^2 \theta \mathcal{H}_{LP} + \frac{3}{4} \sin^2 \theta \mathcal{H}_P + \frac{3}{2} \mathcal{H}_{SP} - 3 \cos \theta \mathcal{H}_{SLP} \right) \left. \right] \\ &+ \alpha_B \sin \theta_B \cos \chi \left[\mp \frac{3}{2\sqrt{2}} \sin \theta \mathcal{H}_{LT} + \frac{3}{4\sqrt{2}} \sin 2\theta \mathcal{H}_{LTP} \right. \\ &+ \delta_\ell \left(-\frac{3}{2\sqrt{2}} \sin 2\theta \mathcal{H}_{LTP} + \frac{3}{\sqrt{2}} \sin \theta \mathcal{H}_{STP} \right) \left. \right\}, \end{aligned} \quad (47)$$

where the polarization asymmetry α_B of the decay $\Lambda_c^+ \rightarrow \Lambda^0 + \pi^+$ is defined by

$$\alpha_B = \frac{|h_{+\frac{1}{2}0}^B|^2 - |h_{-\frac{1}{2}0}^B|^2}{|h_{+\frac{1}{2}0}^B|^2 + |h_{-\frac{1}{2}0}^B|^2}. \quad (48)$$

In order to be able to also discuss the decays $\Lambda_c^+ \rightarrow \Lambda^0 + \ell^+ + \nu_\ell$ and $\bar{\Lambda}_b^0 \rightarrow \bar{\Lambda}_c^- + \ell^+ + \nu_\ell$, we have included the necessary sign changes in Eq. (47). The upper sign refers to the lepton configuration $(\ell^-, \bar{\nu}_\ell)$, and the lower sign refers to the (ℓ^+, ν_ℓ) configuration. The changes are effected by replacing $d_{\lambda_W, \lambda_\ell - 1/2}^J(\theta) \rightarrow d_{\lambda_W, \lambda_\ell + 1/2}^J(\theta)$ and $h_{\lambda_\ell, \lambda_{\bar{\nu}_\ell = 1/2}} \rightarrow h_{\lambda_\ell, \lambda_{\nu_\ell = -1/2}}$ in Eq. (45). The sign changes in Eq.(47) can be seen to result from the parity-violating contribution of the lepton tensor, as discussed in Appendix A.

Let us briefly pause to discuss the cascade decay $\bar{\Lambda}_b^0 \rightarrow \bar{\Lambda}_c^- (\rightarrow \bar{\Lambda}^0 + \pi^-) + \ell^+ + \nu_\ell$ and how the angular decay distribution of the charge conjugated mode is related to that of $\Lambda_b^0 \rightarrow \Lambda_c^+ (\rightarrow \Lambda^0 + \pi^+) + \ell^- + \bar{\nu}_\ell$. We exploit the CP properties of the relevant helicity structure functions. One has

$$\mathcal{H}_X^{\text{pc/pv}}(\bar{\Lambda}_b) = \pm \mathcal{H}_X^{\text{pc/pv}}(\Lambda_b) \quad \text{and} \quad \alpha_{\bar{B}} = -\alpha_B. \quad (49)$$

This shows that the angular decay distribution of the charge conjugated mode is identical to the original mode as long as one replaces the particles in the decay chain $\Lambda_b^0 \rightarrow \Lambda_c^+(\rightarrow \Lambda + \pi^+) + \ell^- + \bar{\nu}_\ell$ with their charge conjugates.

Equation (47) contains 11 distinct helicity structure functions which can be measured by an angular analysis of the cascade decay $\Lambda_b^0 \rightarrow \Lambda_c^+(\rightarrow \Lambda^0 + \pi^+) + W_{\text{off-shell}}^- (\rightarrow \ell^- + \bar{\nu}_\ell)$. Some of the helicity structure functions multiply the same angular factors. To separate them, one also has to take into account the dependence on the factor $\delta_\ell(q^2)$.

In Eq. (43) we have summed over the helicity labels of the lepton; i.e., we have taken the trace of the respective spin density matrix. By leaving the respective helicity labels unsummed, one can then obtain the (θ, θ_B, χ) -dependent polarization of the lepton including the result Eq. (42) after integrating Eq. (45) over $\cos\theta$, $\cos\theta_B$ and χ .

Using the narrow width approximation for the intermediate baryon state Λ_c^+ one finally obtains

$$\begin{aligned} \frac{d\Gamma(\Lambda_b^0 \rightarrow \Lambda_c^+(\rightarrow \Lambda\pi^+) + \ell\bar{\nu}_\ell)}{dq^2 d\cos\theta d\chi d\cos\theta_B} &= \frac{1}{2} \frac{1}{2\pi} \text{Br}(\Lambda_c^+ \rightarrow \Lambda + \pi^+) \Gamma_0 \frac{(q^2 - m_\ell^2)^2 |\mathbf{p}_2|}{M_1^7 q^2} \\ &\times W(\theta) \left(1 + P_z^h(\theta) \alpha_B \cos\theta_B + P_x^h(\theta) \alpha_B \sin\theta_B \cos\chi \right), \end{aligned} \quad (50)$$

where we have factored out the unpolarized rate expression $W(\theta) = 3/8 (2q^2 v^2)^{-1} H^{\mu\nu} L_{\mu\nu}(\theta)$ defined in Eq. (30). $P_z^h(\theta)$ and $P_x^h(\theta)$ are the θ -dependent hadron-side polarization components which read

$$\begin{aligned} P_z^h(\theta) &= \frac{1}{W(\theta)} \left[\frac{3}{8} (1 + \cos^2\theta) \mathcal{H}_P \mp \frac{3}{4} \cos\theta \mathcal{H}_U + \frac{3}{4} \sin^2\theta \mathcal{H}_{LP} \right. \\ &\quad \left. + \delta_\ell \left(\frac{3}{2} \cos^2\theta \mathcal{H}_{LP} + \frac{3}{4} \sin^2\theta \mathcal{H}_P + \frac{3}{2} \mathcal{H}_{SP} - 3 \cos\theta \mathcal{H}_{SLP} \right) \right], \\ P_x^h(\theta) &= \frac{1}{W(\theta)} \left[\mp \frac{3}{2\sqrt{2}} \sin\theta \mathcal{H}_{LT} + \frac{3}{4\sqrt{2}} \sin 2\theta \mathcal{H}_{LTP} + \delta_\ell \left(-\frac{3}{2\sqrt{2}} \sin 2\theta \mathcal{H}_{LTP} + \frac{3}{\sqrt{2}} \sin\theta \mathcal{H}_{STP} \right) \right]. \end{aligned} \quad (51)$$

When integrating the polarization components $P_z^h(\theta)$ and $P_x^h(\theta)$ in Eq. (51) (numerator and denominator separately), one recovers the corresponding expressions in Eq. (41).

Since our model amplitudes are real, and since we are not considering CP -violating effects inasmuch as V_{cb} is real, we have omitted a possible contribution proportional to $P_y(\theta) \alpha_B \sin\theta_B \sin\chi$ in the second line of the distribution (50). The perpendicular polarization component $P_y(\theta)$ is contributed to by the absorptive counterparts of the dispersive structure functions \mathcal{H}_{LT} , \mathcal{H}_{LTP} and \mathcal{H}_{STP} . They are $\text{Im}(H_{+\frac{1}{2}+1} H_{-\frac{1}{2}0}^\dagger + H_{+\frac{1}{2}0} H_{-\frac{1}{2}-1}^\dagger)$, $\text{Im}(H_{+\frac{1}{2}+1} H_{-\frac{1}{2}0}^\dagger - H_{+\frac{1}{2}0} H_{-\frac{1}{2}-1}^\dagger)$ and $\text{Im}(H_{+\frac{1}{2}+1} H_{-\frac{1}{2}t}^\dagger - H_{+\frac{1}{2}t} H_{-\frac{1}{2}-1}^\dagger)$, including also possible CP -odd phases. The three absorptive observables correspond to T -odd observables. The angular factors projecting onto them can be seen to correspond to T -odd momentum products (see Ref. [33]). We emphasize that there are no absorptive parts originating from our two-loop calculation since we have incorporated confinement from the beginning; i.e., the perpendicular polarization component $P_y(\theta)$ is zero in our model.

The last term in the round bracket of Eq. (50) proportional to $P_x^h(\theta)$ describes the azimuthal dependence of the decay rate. After $\cos\theta_B$ - and $\cos\theta$ -integration Eq. (50) allows one to define an azimuthal asymmetry parameter

$$\frac{d\Gamma}{dq^2 d\chi} \propto (1 + \alpha_B \gamma(q^2) \cos\chi) \quad (52)$$

where

$$\gamma(q^2) = -\frac{3\pi^2}{16\sqrt{2}} \frac{(\mathcal{H}_{LT} - 2\delta_\ell \mathcal{H}_{STP})}{\mathcal{H}_{tot}} = \frac{\pi}{4} P_z^h(q^2). \quad (53)$$

The advantage of the $\Lambda_c^+ \rightarrow \Lambda^0 + \pi^+$ mode discussed in this section is that its analyzing power is close to maximal with $\alpha_B = -0.91 \pm 0.15$ [39]. A disadvantage of this mode is that the Λ^0 is rather long lived, with a lifetime of $\tau_\Lambda = 2.63 \cdot 10^{-10} s$ [39], meaning that at the LHC many of the final state Λ 's decay outside of the e.g. LHCb detector such that the decays $\Lambda^0 \rightarrow p\pi^-, n\pi^0$ cannot always be reconstructed. This will become even worse in run 2 of the LHC when the energy, and thus the average energy of the final-state Λ 's, will increase. The optimal place to look for the decay chain $\Lambda_b \rightarrow \Lambda_c \rightarrow \Lambda$ would be for Λ_b 's produced at the GigaZ@ILC option.

Other decay channels of the Λ_c with comparable branching ratios larger than 1% are $\Lambda_c \rightarrow \Lambda \ell^+ \nu$ (-0.86 ± 0.04 [39]), $p\bar{K}^0$ (-1 [40]), $\Sigma^+ \pi^0$ ($-0, 45 \pm 0.31 \pm 0.06$ [39]; 0.71 [40]), $\Sigma^0 \pi^+$ ($+0.70$ [40]), $p\bar{K}^{*0}$ ($+0, 69$ [41]), $pK^-\pi^+$, $\Lambda\rho^+$, $\Sigma^+ \rho^0$, $\Sigma^0 \rho^+$. We have added experimental values (with errors) and theoretical values (without errors) for the respective polarization asymmetry parameters when available. The analyzing power of some of these other modes is not as large as that of the $\Lambda_c^+ \rightarrow \Lambda^0 + \pi^+$ mode but may still lead to reliable measurements of the longitudinal polarization of the Λ_c^+ .

VI The transition form factors in the covariant confined quark model

We shall use the covariant confined quark model previously developed by us to describe the dynamics of the current-induced $\Lambda_b = (b[ud])$ to $\Lambda_c = (c[ud])$ transition (see Refs. [25, 26, 42]). The starting point of the model is an interaction Lagrangian which describes the coupling of the Λ_Q -baryon to the relevant interpolating three-quark current. One has

$$\begin{aligned}\mathcal{L}_{\text{int}}^{\Lambda_Q}(x) &= g_{\Lambda_Q} \bar{\Lambda}_Q(x) \cdot J_{\Lambda_Q}(x) + g_{\Lambda_Q} \bar{J}_{\Lambda_Q}(x) \cdot \Lambda_Q(x), \\ J_{\Lambda_Q}(x) &= \int dx_1 \int dx_2 \int dx_3 F_{\Lambda_Q}(x; x_1, x_2, x_3) J_{3q}^{(\Lambda_Q)}(x_1, x_2, x_3), \\ J_{3q}^{(\Lambda_Q)}(x_1, x_2, x_3) &= \epsilon^{a_1 a_2 a_3} Q^{a_1}(x_1) u^{a_2}(x_2) C \gamma^5 d^{a_3}(x_3), \\ \bar{J}_{\Lambda_Q}(x) &= \int dx_1 \int dx_2 \int dx_3 F_{\Lambda_Q}(x; x_1, x_2, x_3) \bar{J}_{3q}^{(\Lambda_Q)}(x_1, x_2, x_3), \\ \bar{J}_{3q}^{(\Lambda_Q)}(x_1, x_2, x_3) &= \epsilon^{a_1 a_2 a_3} \bar{d}^{a_3}(x_3) \gamma^5 C \bar{u}^{a_2}(x_2) \cdot \bar{Q}^{a_1}(x_1).\end{aligned}\tag{54}$$

The vertex function F_{Λ_Q} is chosen to be of the form

$$F_{\Lambda_Q}(x; x_1, x_2, x_3) = \delta^{(4)}(x - \sum_{i=1}^3 w_i x_i) \Phi_{\Lambda} \left(\sum_{i < j} (x_i - x_j)^2 \right)\tag{55}$$

where Φ_{Λ_Q} is a correlation function involving the three constituent quarks with coordinates x_1, x_2, x_3 and with masses m_1, m_2, m_3 . The variable w_i is defined by $w_i = m_i/(m_1 + m_2 + m_3)$ such that $\sum_{i=1}^3 w_i = 1$. The form factors describing the $\Lambda_Q \rightarrow \Lambda_{Q'}$ transition via the local weak quark current are calculated in terms of a two-loop Feynman diagram. Due to the confinement mechanism of the model, the Feynman diagrams do not contain branch points corresponding to on-shell quark production.

The values of the constituent quark masses m_q are taken from a new fit which improves the description of new data on the exclusive B -meson and the Λ_c decays. In the fit, the infrared cutoff parameter λ of the model has been kept fixed. One has

m_u	m_s	m_c	m_b	λ	
0.241	0.428	1.67	5.04	0.181	GeV

(56)

The values of the size parameters are taken from our previous papers [25, 26]:

Λ_{Λ_s}	Λ_{Λ_c}	Λ_{Λ_b}	
0.492	0.867	0.571	GeV

(57)

The results of our numerical two-loop calculation are well represented by a double-pole parametrization

$$F(q^2) = \frac{F(0)}{1 - as + bs^2}, \quad s = \frac{q^2}{M_1^2}\tag{58}$$

with high accuracy: the relative error is less than 1%. In Fig. 2 we display a comparison of the exact results for the relativistic form factors F_i^V and F_i^A ($i = 1, 2, 3$) with the double-pole parametrization. For the $\Lambda_b \rightarrow \Lambda_c$ transition the parameters of the approximated form of the form factors are given by

	F_1^V	F_2^V	F_3^V	F_1^A	F_2^A	F_3^A
$F(0)$	0.549	0.110	-0.023	0.542	0.018	-0.123
a	1.459	1.680	1.181	1.443	0.921	1.714
b	0.571	0.794	0.276	0.559	0.255	0.828

(59)

The dominant form factors are $F_1^V(q^2)$ and $F_1^A(q^2)$ with very similar q^2 dependencies. Inasmuch as one can neglect the other form factors, the results of our model calculation are very close to the leading-order HQET result $F_1^V(q^2) = F_1^A(q^2) = F(q^2)$, $F_{2,3}^{V/A} = 0$ discussed in Sec. II. In fact, our numerical results to be discussed in Sec. VII are quite close to what would be expected in leading-order HQET.

Let us take a closer look at the q^2 dependence of the form factors $F_1^V(q^2) \approx F_1^A(q^2)$. Their q^2 dependence is very close to a dipole behavior, since one has $\sqrt{b} \sim a/2$ in both cases with a dipole mass $m_{\text{dipole}} = M_1/\sqrt{a/2} \sim 6.6$ GeV. The dipole mass is quite close to the expected $(b\bar{c})$ mass scale of 6.28 GeV set by the B_c -meson mass [39]. Next, we look at the near zero recoil behavior of $F_1^V(q^2)$ and $F_1^A(q^2)$. In order to investigate the near recoil zero behavior of the form factors, we switch to the variable $w = (M_1^2 + M_2^2 - q^2)/(2M_1M_2)$ such that $w = 1$ at the zero recoil point $q^2 = q_{\text{max}}^2 = (M_1 - M_2)^2$. The Taylor expansion of any given function $f(w)$ around the zero recoil point $w = 1$ reads

$$\begin{aligned} f(w) &= \sum_{n=0}^{\infty} \frac{f^{(n)}}{n!} (w-1)^n \\ &= f(1) \left\{ 1 + \frac{f'(1)}{f(1)}(w-1) + \frac{f''(1)}{2f(1)}(w-1)^2 + \dots \right\} \\ &\equiv f(1) \left\{ 1 - \rho^2(w-1) + c(w-1)^2 + \dots \right\} \end{aligned} \quad (60)$$

where ρ^2 is called the slope parameter and c is the convexity parameter. It is not difficult to express the parameters $f(w=1)$, ρ^2 and c via the original parameters $F(0)$, a and b used in the double-pole parametrization Eq. (58). One finds

$$\begin{aligned} f(w=1) &= \frac{F(0)}{1 - a s_{\text{max}} + b s_{\text{max}}^2}, \\ \rho^2 &= \frac{2r(a - 2b s_{\text{max}})}{1 - a s_{\text{max}} + b s_{\text{max}}^2}, \quad c = \frac{4r^2 [a^2 - b - 3ab s_{\text{max}} + 3b^2 s_{\text{max}}^2]}{[1 - a s_{\text{max}} + b s_{\text{max}}^2]^2} \end{aligned} \quad (61)$$

where $r = M_2/M_1$ and $s_{\text{max}} = (1 - r)^2$. The numerical results for $F_1^V(q^2)$ and $F_1^A(q^2)$ can be calculated to be

	$f(w=1)$	ρ^2	c
F_1^V	0.985	1.543	1.704
F_1^A	0.966	1.521	1.654

First, one notes that the zero recoil normalization is very close to 1 for both F_1^V and F_1^A , which would be the normalization predicted by leading order HQET. The values for the two slope parameters are compatible with the only experimental result published by the DELPHI Collaboration: $\rho^2 = 2.03 \pm 0.46(\text{stat})_{-1.00}^{+0.72}(\text{syst})$ [43]. There are no experimental results on the convexity parameter yet. There are a number of theoretical model calculations for the slope parameter of the $\Lambda_b \rightarrow \Lambda_c$ transitions, many of which scatter around $\rho^2 \approx 1.5$ [44–52]. A value around 1.5 is expected from the spectator quark model relation $\rho_B^2 = 2\rho_M^2 - 1/2$ [53] using a mesonic slope parameter of $\rho_M^2 \approx 1$ as reported by the Heavy Flavor Averaging Group [54].

VII Numerical results

We shall present numerical results for the two cases $\ell^- = e^-$ and $\ell^- = \tau^-$. The results for the μ^- mode are almost identical to those of the e^- mode and will not be listed separately. The dynamical input in terms of the covariant confined quark model has been specified in Sec. VI. We use the mass values $M_{\Lambda_b} = 5.6195$ GeV, $M_{\Lambda_c} = 2.2864$ GeV and $m_\tau = 1.7768$ GeV [39].

In Fig. 3, we display the q^2 dependence of the partial differential rates $d\Gamma_U/dq^2$, $d\Gamma_L/dq^2$ and the total differential rate $d\Gamma_{U+L}/dq^2$ for the e mode. The transverse rate dominates in the low recoil region while the longitudinal rate dominates in the large recoil region. The longitudinal and thereby the total rate shows a step-like behavior close to the threshold $q^2 = m_e^2$. Figure 4 shows the corresponding plots for the τ mode including the partial flip rates $d\tilde{\Gamma}_{U,L}/dq^2$ and $3d\tilde{\Gamma}_S/dq^2$. We also show the total differential rate $(d\Gamma_{U+L}/dq^2 + d\tilde{\Gamma}_{U+L+3S}/dq^2)$. The behavior of

the longitudinal and scalar partial flip rates can be seen to be quite close to the HQET result $d\tilde{\Gamma}_L/dq^2 = d\tilde{\Gamma}_S/dq^2$. The helicity flip rates are smaller than the helicity nonflip rates but contribute significantly to the total rate.

In Fig. 5, we show the q^2 dependence of the lepton-side forward-backward asymmetry $A_{FB}^\ell(q^2)$ defined in Eq. (38). At zero recoil, $A_{FB}^\ell(q^2)$ approaches zero for both the e and τ modes due to the zero recoil relations $\mathcal{H}_P = \mathcal{H}_{SL} = 0$ [see Eq. (12)]. In the large recoil limit, $A_{FB}^\ell(e)$ goes to zero due to the longitudinal dominance of the partial rates. The q^2 dependence of the forward-backward asymmetry of the two modes is distinctly different. While $A_{FB}^\ell(e)$ remains positive in the whole q^2 range, $A_{FB}^\ell(\tau)$ quickly becomes negative when moving away from zero recoil. It is interesting to observe that $A_{FB}^\ell(\tau)$ goes through a zero at $q^2 \approx 8 \text{ GeV}^2$.

In Fig. 6, we display the q^2 dependence of the convexity parameter C_F defined in Eq. (39). At zero recoil, C_F goes to zero for both modes due to the zero recoil relation $\mathcal{H}_U = 2\mathcal{H}_L$ [see Eq. (12)]. For the e mode, one finds $C_F \rightarrow -1, 5$ at maximal recoil due to longitudinal dominance, while $C_F \rightarrow 0$ for the τ mode at maximal recoil $q^2 = m_\tau^2$ due to the overall factor $(1 - 2\delta)$ in Eq. (39). In the τ mode, the convexity parameter remains quite small over the whole accessible q^2 range, implying a near straight-line behavior of the $\cos\theta$ distribution. In the e mode C_F can become large and negative, which implies that the $\cos\theta$ distribution is strongly parabolic in terms of a downward open tilted parabola.

In Figs. 7 and 8 we show the longitudinal and transverse polarization components of the Λ_c defined in Eq. (41). For the e mode the longitudinal polarization goes to zero at zero recoil since $\mathcal{H}_P = \mathcal{H}_{LP} = \mathcal{H}_{SP} = 0$ at zero recoil [see Eq. (12)]. At maximal recoil, P_z^h goes to zero for both modes because of the HQET plus $q^2 = 0$ relation Eq. (17). The two e and τ curves almost fall on top of each other in their common q^2 range. The zero recoil values of the transverse polarization P_x^h in Fig. 8 can be understood in terms of the zero recoil limit of HQET [see Eq. (16)]. At zero recoil, one has $P_x \rightarrow -(\pi/4)(1 - 2\delta_\ell)/(1 + 2\delta_\ell) = (-0.79; -0.43)$, which is in approximative agreement with what is shown in Fig. 8. At minimal recoil, one has $P_x^h = 0$ for both the e and the τ modes. For the τ mode, this can be understood from the approximate validity of HQET (see the fourth equation in Eq. (16) together with the fact that $\delta_\ell = 1/2$ at $q^2 = m_\tau^2$). For the e mode, one has $P_x^h = 0$ at zero recoil which follows from longitudinal dominance at zero recoil. The transverse polarization is considerably reduced going from the e mode to the τ -mode. The magnitude of the Λ_c polarization shown in Fig. 9 is quite large for the e -mode and smaller for the τ -mode. The maximal recoil values reflect the corresponding dP_x^h/dq^2 limits in Fig. 8, since the z -components are zero at maximal recoil.

In Figs. 10 and 11, we show the q^2 dependence of the longitudinal and transverse polarization component of the charged lepton. In the case of the electron, the two curves reflect the chiral limit of a massless lepton in which the lepton is purely left-handed. The behavior of the two polarization components in the τ mode is distinctly different. The longitudinal polarization is reduced from -1 , while the transverse polarization can become quite large towards maximal recoil. At zero recoil, the transverse polarization of the charged lepton P_x^T tends to zero in agreement with the vanishing of \mathcal{H}_P and \mathcal{H}_{SL} at zero recoil [see Eq. (12)]. The total polarization of the lepton shown in Fig. 12 is maximal in the e mode and somewhat reduced but still quite large in the τ -mode.

Below we present our predictions for the semileptonic branching ratios of the Λ_b and Λ_c and compare them with data. Consideration of both modes is sufficient to fix the model parameters of the Λ_c — constituent quark mass m_c and the size parameter Λ_{Λ_c} . We have used the value for the Λ_b lifetime from the new edition of the Particle Data Group (PDG) [39] $\tau_{\Lambda_b} = (1.451 \pm 0.013) \cdot 10^{-12} \text{ s}$. We have also followed the recommendation of the PDG and have rescaled the branching ratio $\text{Br}(\Lambda_c^+ \rightarrow \Lambda^0 + e^+ \nu_e)$ upward by 30 %, taking into account the new absolute measurement of $\text{Br}(\Lambda_c^+ \rightarrow pK^- \pi^+)$ by the Belle Collaboration [55]. We thus use a branching ratio $\text{Br}(\Lambda_c^+ \rightarrow \Lambda^0 + e^+ \nu_e) = (2.74 \pm 0.82)\%$ instead of $\text{Br}(\Lambda_c^+ \rightarrow \Lambda^0 + e^+ \nu_e) = (2.1 \pm 0.6)\%$ as listed in the 2014 edition of the PDG.

Mode	Our results	Data
$\Lambda_c^+ \rightarrow \Lambda^0 e^+ \nu_e$	2.72	2.74 ± 0.82
$\Lambda_b^0 \rightarrow \Lambda_c^+ e^- \bar{\nu}_e$	6.9	$6.5_{-2.5}^{+3.2}$
$\Lambda_b^0 \rightarrow \Lambda_c^+ \tau^- \bar{\nu}_\tau$	2.0	

(63)

The numbers in Table II show again that the results of our dynamical calculation are very close to the HQET results $\tilde{\Gamma}_L = \tilde{\Gamma}_S = -\tilde{\Gamma}_{SLP}$, $\tilde{\Gamma}_{SP} = \tilde{\Gamma}_{LP} = -\tilde{\Gamma}_{SL}$ and $\tilde{\Gamma}_{STP} = \tilde{\Gamma}_{LT}$ given in terms of the helicity structure functions in Eq. (15). Note, though, that the agreement with leading-order HQET is of effective nature only since e.g. the size parameters of the Λ_b and the Λ_c are quite different [see Eq. (57)].

From the partial rates in Table II, we can compile the total rate. Again, we list the partial and total rates in units

TABLE II: q^2 averages of helicity structure functions in units of 10^{-15} GeV. We do not display helicity flip results for the e mode, because they are of order $10^{-6} - 10^{-7}$ in the above units.

	Γ_U	Γ_L	Γ_{LT}			Γ_P	Γ_{LP}	Γ_{LTP}			
e	12.4	19.6	-7.73			-7.61	-18.5	-3.50			
τ	3.29	2.90	-2.06			-1.73	-2.46	-0.66			
	$\tilde{\Gamma}_U$	$\tilde{\Gamma}_L$	$\tilde{\Gamma}_S$	$\tilde{\Gamma}_{LT}$	$\tilde{\Gamma}_{SP}$	$\tilde{\Gamma}_{SL}$	$\tilde{\Gamma}_P$	$\tilde{\Gamma}_{LP}$	$\tilde{\Gamma}_{LTP}$	$\tilde{\Gamma}_{STP}$	$\tilde{\Gamma}_{SLP}$
τ	0.66	0.63	0.64	-0.41	-0.55	0.55	-0.37	-0.55	-0.14	-0.42	-0.64

of 10^{-15} GeV. One has

	Γ_U	Γ_L	$\tilde{\Gamma}_U$	$\tilde{\Gamma}_L$	$3\tilde{\Gamma}_S$	Γ_{tot}
$e^- \bar{\nu}_e$	12.4	19.6	32.0
$\tau^- \bar{\nu}_\tau$	3.29	2.90	0.66	0.63	1.92	9.40

(64)

The numbers show that the partial flip rates make up 34.2% of the total rate, where the biggest contribution comes from the scalar rate with 20.4%.

Next, we give the values of the integrated quantities — forward-backward asymmetry $\langle A_{FB} \rangle$, the asymmetry parameter $\langle \alpha \rangle$, the convexity parameter $\langle C_F \rangle$, and the hadronic $\langle P_{x,z}^h \rangle$ and leptonic $\langle P_{x,z}^\ell \rangle$ polarization components calculated in the model. These can be obtained from the nonflip and flip rates collected in Table II. For example, one has

$$\langle A_{FB}^\ell \rangle = -\frac{3}{2} \frac{\Gamma_P + 4\tilde{\Gamma}_{SL}}{\Gamma_{tot}} \quad \langle \alpha \rangle = \langle P_z \rangle = \frac{\Gamma_P + \Gamma_{LP} + \tilde{\Gamma}_{LP} + \tilde{\Gamma}_P + 3\tilde{\Gamma}_{SP}}{\Gamma_{tot}} \quad . \quad (65)$$

	$\langle A_{FB}^\ell \rangle$	$\langle C_F \rangle$	$\langle P_z^h \rangle$	$\langle P_x^h \rangle$	$\langle P_z^\ell \rangle$	$\langle P_x^\ell \rangle$	$\langle \gamma \rangle$
$e^- \bar{\nu}_e$	0.36	-0.63	-0.82	0.40	-1.00	0.00	0.31
$\tau^- \bar{\nu}_\tau$	-0.077	-0.10	-0.72	0.22	-0.32	0.55	0.17

(66)

Note that the mean of the azimuthal asymmetry parameter $\langle \gamma \rangle$ defined in (52) is related to $\langle P_x^h \rangle$ by $\langle \gamma \rangle = (\pi/4) \langle P_x^h \rangle$. When calculating the q^2 averages one has to remember to include the q^2 dependent factor $(q^2 - m_\ell^2)^2 |\mathbf{p}_2|/q^2$ in the numerator and denominator of the relevant asymmetry expressions. In most of the shown cases, the mean values change considerably when going from the e to the τ modes including even a sign change in $\langle A_{FB}^\ell \rangle$.

VIII Summary and conclusions

Let us summarize the main results of our paper. We have used the helicity formalism to study the angular decay distribution in the semileptonic decay $\Lambda_b^0 \rightarrow \Lambda_c^+ + \ell^- \bar{\nu}_\tau$ as well as the corresponding cascade decay $\Lambda_b^0 \rightarrow \Lambda_c^+ (\rightarrow \Lambda^0 + \pi^+) + \ell^- \bar{\nu}_\tau$. Starting from the angular decay distribution, we have defined a number of polarization observables, for which we have provided numerical results using form factors obtained in the covariant confined quark model. All our results have been presented for the two cases (i) the near mass zero leptons $\ell = e, \mu$ and (ii) the massive τ lepton $\ell = \tau$. We have demonstrated the case with which lepton mass effects can be included in the helicity formalism. The numerical results for the polarization observables are given in the form of q^2 plots and also in

averaged form, where the average has been taken with regard to the lepton-side polar angle $\cos\theta$ and also with regard to q^2 . We find substantial lepton mass effects in most of the polarization observables. We have also discussed the decay $\bar{\Lambda}_b^0 \rightarrow \bar{\Lambda}_c^- (\rightarrow \bar{\Lambda}^0 + \pi^-) + \ell^+ \nu_\ell$, the angular decay distribution of which is identical to that of the decay $\Lambda_b^0 \rightarrow \Lambda_c^+ (\Lambda^0 + \pi^+) + \ell^- \bar{\nu}_\ell$ after implementing the appropriate changes. In our analysis we have assumed that the parent baryon Λ_b is unpolarized. The case of polarized Λ_b decays would bring in a number of new polarization observables as discussed in corresponding calculations in Refs. [26, 33, 35].

In our analysis we have remained within the SM. The helicity formalism for the decays presented in this paper easily allows one to include effects beyond the BSM. A generic charged Higgs contribution would populate the scalar helicity amplitudes $H_{+\frac{1}{2}t}^{V/A}$ and would thus affect the helicity structure functions \mathcal{H}_S , \mathcal{H}_{SL} , \mathcal{H}_{SP} , and \mathcal{H}_{STP} through their interference with the SM contributions. Tensor currents contribute only to the spin-1 piece of the helicity amplitudes $H_{+\frac{1}{2}+1}^{V/A}$ and $H_{+\frac{1}{2}0}^{V/A}$. They would populate all helicity structure functions when interfering with the SM amplitudes except for \mathcal{H}_S . Depending on the chiral structure of the lepton-side effective currents, the pattern of helicity flip and nonflip contributions to the helicity structure functions would be redistributed. It would be interesting to find out how many of the BSM proposals that have been introduced in the meson sector to explain the tensions with the SM results would have a measurable effect in the baryon sector.

Acknowledgments

This work was supported by the Tomsk State University Competitiveness Improvement Program. M.A.I. acknowledges the support from the Mainz Institute for Theoretical Physics (MITP). M.A.I. and J.G.K. thank the Heisenberg-Landau Grant for support.

A Unpolarized and polarized lepton tensor

In this appendix we determine the helicity components of the unpolarized and polarized lepton tensor in the Λ_b decay system (z axis along the momentum of the off-shell W) using covariant methods. As shown in Eq. (44) the unpolarized and polarized helicity components in the Λ_b decay system can also be obtained by a rotation of the helicity components of the lepton tensor in the W -decay system (z axis along ℓ^\mp). This provides for a check of the covariant calculation. In the following, the helicity components of the lepton tensor are always given for both the $(\ell^- \bar{\nu}_\ell)$ and the $(\ell^+ \nu_\ell)$ configurations. The latter configuration is needed for the decay $\bar{\Lambda}_b^0 \rightarrow \bar{\Lambda}_c^- + \ell^+ \nu_\ell$ or for the decay $\Lambda_c^+ \rightarrow \Lambda^0 + \ell^+ \nu_\ell$.

1. Unpolarized lepton

The unpolarized lepton tensor for the process $W_{\text{off-shell}}^- \rightarrow \ell^- \bar{\nu}_\ell$ ($W_{\text{off-shell}}^+ \rightarrow \ell^+ \nu_\ell$) is calculated as

$$\begin{aligned} L^{\mu\nu} &= \begin{cases} \text{tr} \left[(\not{p}_\ell + m_\ell) \gamma^\mu (1 - \gamma_5) \not{p}_{\nu_\ell} \gamma^\nu (1 - \gamma_5) \right] & \text{for } W_{\text{off-shell}}^- \rightarrow \ell^- \bar{\nu}_\ell \\ \text{tr} \left[(\not{p}_\ell - m_\ell) \gamma^\nu (1 - \gamma_5) \not{p}_{\nu_\ell} \gamma^\mu (1 - \gamma_5) \right] & \text{for } W_{\text{off-shell}}^+ \rightarrow \ell^+ \nu_\ell \end{cases} \\ &= 8 \left(p_\ell^\mu p_{\nu_\ell}^\nu + p_\ell^\nu p_{\nu_\ell}^\mu - p_\ell \cdot p_{\nu_\ell} g^{\mu\nu} \pm i \varepsilon^{\mu\nu\alpha\beta} p_{\ell\alpha} p_{\nu_\ell\beta} \right) \end{aligned} \quad (\text{A1})$$

where the upper/lower sign refers to the two $(\ell^- \bar{\nu}_\ell)/(\ell^+ \nu_\ell)$ configurations. The sign change can be seen to result from the p.v. part of the lepton tensors.

We shall evaluate the lepton tensor components in the $W_{\text{off-shell}}$ rest frame with the z -axis along the original momentum direction of the $W_{\text{off-shell}}$ (see Fig. 1). The polarization four-vectors in the $W_{\text{off-shell}}$ rest frame with helicities $\lambda_W = t, \pm, 0$ are given by

$$\epsilon^\mu(t) = (1, 0, 0, 0) \quad \epsilon^\mu(\pm) = \frac{1}{\sqrt{2}}(0, \mp 1, -i, 0) \quad \epsilon^\mu(0) = (0, 0, 0, 1). \quad (\text{A2})$$

The momentum vectors p_ℓ^μ and p_{ν_ℓ} in the same system read (see Fig. 1)

$$p_\ell^\mu = (E_\ell; |\mathbf{p}_\ell| \sin \theta \cos \chi, |\mathbf{p}_\ell| \sin \theta \sin \chi, |\mathbf{p}_\ell| \cos \theta), \quad p_{\nu_\ell}^\mu = |\mathbf{p}_\ell| (1; -\sin \theta \cos \chi, -\sin \theta \sin \chi, -\cos \theta), \quad (\text{A3})$$

where $E_\ell = (q^2 + m_\ell^2)/(2\sqrt{q^2})$ and $|\mathbf{p}_\ell| = (q^2 - m_\ell^2)/(2\sqrt{q^2}) = \sqrt{q^2}v/2$ are the energy and momenta of the charged lepton. The helicity components $L_{\lambda_W \lambda'_W}(\theta, \chi)$ can then be obtained from the contraction

$$L_{\lambda_W \lambda'_W}(\theta, \chi) = L^{\mu\nu}(\theta, \chi) \epsilon_\mu(\lambda_W) \epsilon_\nu^*(\lambda'_W) \quad (\text{A4})$$

One obtains (the rows and columns of the matrix are ordered in the sequence $(t, 1, 0, -1)$)

$$(2q^2v)^{-1} L_{\lambda_W \lambda'_W}(\theta, \chi) = \begin{pmatrix} 0 & 0 & 0 & 0 \\ 0 & (1 \mp \cos \theta)^2 & \mp \frac{2}{\sqrt{2}}(1 \mp \cos \theta) \sin \theta e^{i\chi} & \sin^2 \theta e^{2i\chi} \\ 0 & \mp \frac{2}{\sqrt{2}}(1 \mp \cos \theta) \sin \theta e^{-i\chi} & 2 \sin^2 \theta & \mp \frac{2}{\sqrt{2}}(1 \pm \cos \theta) \sin \theta e^{i\chi} \\ 0 & \sin^2 \theta e^{-2i\chi} & \mp \frac{2}{\sqrt{2}}(1 \pm \cos \theta) \sin \theta e^{-i\chi} & (1 \pm \cos \theta)^2 \end{pmatrix} + \delta_\ell \begin{pmatrix} 4 & -\frac{4}{\sqrt{2}} \sin \theta e^{i\chi} & 4 \cos \theta & \frac{4}{\sqrt{2}} \sin \theta e^{i\chi} \\ -\frac{4}{\sqrt{2}} \sin \theta e^{-i\chi} & 2 \sin^2 \theta & -\frac{2}{\sqrt{2}} \sin 2\theta e^{i\chi} & -2 \sin^2 \theta e^{2i\chi} \\ 4 \cos \theta & -\frac{2}{\sqrt{2}} \sin 2\theta e^{-i\chi} & 4 \cos^2 \theta & \frac{2}{\sqrt{2}} \sin 2\theta e^{i\chi} \\ \frac{4}{\sqrt{2}} \sin \theta e^{-i\chi} & -2 \sin^2 \theta e^{-2i\chi} & \frac{2}{\sqrt{2}} \sin 2\theta e^{-i\chi} & 2 \sin^2 \theta \end{pmatrix} \quad (\text{A5})$$

The components $L_{1-1}(\theta, \chi)$ and $L_{-11}(\theta, \chi)$ are not probed in unpolarized Λ_b decays because of the condition $|\lambda_W - \lambda'_W| \leq 1$ discussed after Eq. (46). These two components are, however, probed in polarized Λ_b decays.

When one integrates Eq. (A5) over the azimuthal angle χ one obtains the quasi-diagonal form

$$\frac{1}{2\pi} (2q^2v)^{-1} L_{\lambda_W \lambda'_W}(\theta) = \begin{pmatrix} 0 & 0 & 0 & 0 \\ 0 & (1 \mp \cos \theta)^2 & 0 & 0 \\ 0 & 0 & 2 \sin^2 \theta & 0 \\ 0 & 0 & 0 & (1 \pm \cos \theta)^2 \end{pmatrix} + \delta_\ell \begin{pmatrix} 4 & 0 & 4 \cos \theta & 0 \\ 0 & 2 \sin^2 \theta & 0 & 0 \\ 4 \cos \theta & 0 & 4 \cos^2 \theta & 0 \\ 0 & 0 & 0 & 2 \sin^2 \theta \end{pmatrix} \quad (\text{A6})$$

where $L_{\lambda_W \lambda'_W}(\theta) = \int d\chi L_{\lambda_W \lambda'_W}(\theta, \chi)$.

Finally, integrating Eq. (A6) over $\cos \theta$ one obtains the diagonal form

$$\frac{1}{2\pi} (2q^2v)^{-1} L_{\lambda_W \lambda'_W} = \frac{8}{3} \begin{pmatrix} 3\delta_\ell & 0 & 0 & 0 \\ 0 & (1 + \delta_\ell) & 0 & 0 \\ 0 & 0 & (1 + \delta_\ell) & 0 \\ 0 & 0 & 0 & (1 + \delta_\ell) \end{pmatrix} \quad (\text{A7})$$

where $L_{\lambda_W \lambda'_W} = \int d\cos \theta L_{\lambda_W \lambda'_W}(\theta)$.

Next we calculate the lepton helicity tensor $\hat{L}_{\hat{\lambda}_W \hat{\lambda}'_W}$ in the W -decay system with the z -axis along the charged lepton. In order to set it apart from the lepton helicity tensor in the Λ_b -decay system, we use a hat notation such that $\hat{\lambda}_W = \lambda_\ell - \lambda_\nu$. The components of $\hat{L}_{\hat{\lambda}_W \hat{\lambda}'_W}$ can be calculated as in (A4), but now using

$$p_\ell^\mu = (E_\ell; 0, 0, |\mathbf{p}_\ell|), \quad p_{\nu_\ell}^\mu = |\mathbf{p}_\ell|(1; 0, 0, -1). \quad (\text{A8})$$

The nonvanishing components read

$$(2q^2v)^{-1} \hat{L}_{\mp\mp} = 4 \quad (2q^2v)^{-1} \hat{L}_{00} = (2q^2v)^{-1} \hat{L}_{t0} = (2q^2v)^{-1} \hat{L}_{0t} = (2q^2v)^{-1} \hat{L}_{tt} = 4\delta_\ell. \quad (\text{A9})$$

The helicity components $L_{\lambda_W \lambda'_W}(\theta, \chi)$ in the Λ_b -decay system can be obtained from the $\hat{L}_{\hat{\lambda}_W \hat{\lambda}'_W}$ in the W -decay system by an appropriate rotation. One has

$$L_{\lambda_W \lambda'_W}(\theta, \chi) = \sum_{\hat{\lambda}_W, \hat{\lambda}'_W = t, \mp 1, 0} d_{\lambda_W, \hat{\lambda}_W}^J(\theta) d_{\lambda'_W, \hat{\lambda}'_W}^{J'}(\theta) e^{i(\lambda_W - \lambda'_W)\chi} \hat{L}_{\hat{\lambda}_W \hat{\lambda}'_W}. \quad (\text{A10})$$

2. Longitudinal polarization P_z^ℓ

Next we calculate the longitudinal polarization component P_z of the charged lepton. The relevant lepton tensor can be obtained from the unpolarized tensor by the substitution $p_\ell^\mu \rightarrow \mp m_\ell s_z^\mu$:

$$L^{\mu\nu}(s_z) = \mp 8m_\ell \left(s_z^\mu p_{\nu_\ell}^\nu + s_z^\nu p_{\nu_\ell}^\mu - s_z \cdot p_{\nu_\ell} g^{\mu\nu} \pm i\varepsilon^{\mu\nu\alpha\beta} s_{z\alpha} p_{\nu_\ell\beta} \right). \quad (\text{A11})$$

At present, we shall not consider the χ dependence of the longitudinal polarization component P_z . Without loss of generality, one can then set $\chi = 0$ in the representation of the momentum $p_{\nu_\ell}^\mu$ in Eq. (A3) but must compensate by the factor 2π from the trivial χ integration. The four-component spin vector s_z^μ reads ($\chi = 0$)

$$s_z^\mu = \frac{1}{m_\ell}(|\mathbf{p}_\ell|; E_\ell \sin \theta, 0, E_\ell \cos \theta) \quad (\text{A12})$$

which satisfies the conditions $s_{z,\mu} s_z^\mu = -1$ and $s_{z,\mu} \cdot p_\ell^\mu = 0$.

The components $L_{\lambda_W \lambda'_W}(s_z; \theta)$ can be calculated to be

$$\begin{aligned} \frac{1}{2\pi} (2q^2 v)^{-1} L_{tt}(s_z; \theta) &= \pm 4\delta_\ell && \rightarrow \pm 8\delta_\ell, \\ \frac{1}{2\pi} (2q^2 v)^{-1} L_{t0}(s_z; \theta) &= \frac{1}{2\pi} (2q^2 v)^{-1} L_{0t}(s_z; \theta) = \pm 4\delta_\ell \cos \theta && \rightarrow 0, \\ \frac{1}{2\pi} (2q^2 v)^{-1} L_{++}(s_z; \theta) &= -(1 \mp \cos \theta)^2 + 2\delta_\ell \sin^2 \theta && \rightarrow \mp \frac{8}{3}(1 - \delta_\ell), \\ \frac{1}{2\pi} (2q^2 v)^{-1} L_{00}(s_z; \theta) &= -2 \sin^2 \theta + 4\delta_\ell \cos^2 \theta && \rightarrow \mp \frac{8}{3}(1 - \delta_\ell), \\ \frac{1}{2\pi} (2q^2 v)^{-1} L_{--}(s_z; \theta) &= -(1 \pm \cos \theta)^2 + 2\delta_\ell \sin^2 \theta && \rightarrow \mp \frac{8}{3}(1 - \delta_\ell). \end{aligned} \quad (\text{A13})$$

The nonvanishing helicity components $\hat{L}_{\hat{\lambda}_W \hat{\lambda}'_W}$ in the W -decay helicity system are obtained by setting $\theta = 0$ in (A12) such that $s_z^\mu = (|\mathbf{p}_\ell|; 0, 0, E_\ell)/m_\ell$ and taking $p_{\nu_\ell}^\mu$ as in (A8). One obtains

$$(2q^2 v)^{-1} \hat{L}_{\mp\mp}(s_z) = \mp 4, \quad (2q^2 v)^{-1} \hat{L}_{00}(s_z) = (2q^2 v)^{-1} \hat{L}_{t0}(s_z) = (2q^2 v)^{-1} \hat{L}_{0t}(s_z) = (2q^2 v)^{-1} \hat{L}_{tt}(s_z) = \pm 4\delta_\ell. \quad (\text{A14})$$

The helicity components $L_{\lambda_W \lambda'_W}(s_z; \theta)$ in the Λ_b -decay system can again be obtained by rotation:

$$\sum_{\hat{\lambda}_W, \hat{\lambda}'_W} L_{\lambda_W \lambda'_W}(s_z, \theta) = \sum_{\hat{\lambda}_W, \hat{\lambda}'_W} d_{\lambda_W \hat{\lambda}_W}^J(\theta) d_{\lambda'_W \hat{\lambda}'_W}^{J'}(\theta) \hat{L}_{\hat{\lambda}_W \hat{\lambda}'_W}(s_z). \quad (\text{A15})$$

3. Transverse polarization P_x^ℓ

The lepton tensor relevant for the transverse polarization P_x of the charged lepton is obtained from the unpolarized expression by the substitution $p_\ell^\mu \rightarrow \mp m_\ell s_x^\mu$. Again we set $\chi = 0$ without loss of generality. The polarized lepton tensor reads

$$L^{\mu\nu}(s_x) = \mp 8m_\ell \left(s_x^\mu p_{\nu_\ell}^\nu + s_x^\nu p_{\nu_\ell}^\mu - s_x \cdot p_{\nu_\ell} g^{\mu\nu} \pm i\varepsilon^{\mu\nu\alpha\beta} s_{x\alpha} p_{\nu_\ell\beta} \right), \quad (\text{A16})$$

where s_x^μ is the four-component spin vector

$$s_x^\mu = (0; \cos \theta, 0, -\sin \theta). \quad (\text{A17})$$

obeying the conditions $s_{x,\mu} s_x^\mu = -1$ and $s_{x,\mu} \cdot p_\ell^\mu = 0$. Just as before, the relevant components of the polarized lepton tensor are obtained by contraction with the relevant polarization four-vectors. One obtains

$$\begin{aligned} \frac{1}{2\pi} (2q^2 v)^{-1} L_{tt}(s_x; \theta) &= 0 && \rightarrow 0, \\ \frac{1}{2\pi} (2q^2 v)^{-1} L_{t0}(s_x; \theta) &= (2q^2 v)^{-1} L_{0t}(s_x; \theta) = \mp \sqrt{\delta_\ell} \frac{4}{\sqrt{2}} \sin \theta && \rightarrow \mp 2\pi \sqrt{\delta_\ell/2}, \\ \frac{1}{2\pi} (2q^2 v)^{-1} L_{++}(s_x; \theta) &= -\sqrt{\delta_\ell} \frac{4}{\sqrt{2}} \sin \theta (1 \mp \cos \theta) && \rightarrow -2\pi \sqrt{\delta_\ell/2}, \\ \frac{1}{2\pi} (2q^2 v)^{-1} L_{00}(s_x; \theta) &= \mp \sqrt{\delta_\ell} \frac{8}{\sqrt{2}} \sin \theta \cos \theta && \rightarrow 0, \\ \frac{1}{2\pi} (2q^2 v)^{-1} L_{--}(s_x; \theta) &= \sqrt{\delta_\ell} \frac{4}{\sqrt{2}} \sin \theta (1 \pm \cos \theta) && \rightarrow +2\pi \sqrt{\delta_\ell/2}. \end{aligned} \quad (\text{A18})$$

The nonvanishing helicity components in the W -decay system are obtained by setting $\theta = 0$ in (A17) such that $s_x^\mu = (0; 1, 0, 0)$. One obtains

$$(2q^2v^2)^{-1}(\hat{L}_{t\mp}) = (2q^2v^2)^{-1}(\hat{L}_{\mp t}) = (2q^2v^2)^{-1}\hat{L}_{0\mp} = (2q^2v^2)^{-1}(\hat{L}_{\mp 0}) = 4\sqrt{\delta_\ell}. \quad (\text{A19})$$

As before the relevant helicity components in the production system are obtained by a rotation via

$$\sum_{\hat{\lambda}_W, \hat{\lambda}'_W} L_{\lambda_W \lambda'_W}(s_x, \theta) = \sum_{\hat{\lambda}_W, \hat{\lambda}'_W} d_{\lambda_W \hat{\lambda}_W}^J(\theta) d_{\lambda'_W \hat{\lambda}'_W}^{J'}(\theta) \hat{L}_{\hat{\lambda}_W \hat{\lambda}'_W}(s_x). \quad (\text{A20})$$

B Lepton-side helicity amplitudes

In this appendix we calculate the lepton-side helicity amplitudes appearing in Eqs. (28), (44) and (45). The lepton-side helicity amplitudes $h_{\lambda_\ell, 1/2}$ for the process $W_{\text{off-shell}}^- \rightarrow \ell^- \bar{\nu}_\ell$ are defined by ($\hat{\lambda}_W = \lambda_\ell - 1/2$)

$$h_{\hat{\lambda}_W; \lambda_{\ell^-}, 1/2}(J) = \bar{u}_{\ell^-}(\lambda_\ell) \gamma_\mu (1 - \gamma_5) v_{\bar{\nu}_\ell}(1/2) \epsilon^\mu(\hat{\lambda}_W). \quad (\text{B1})$$

As before, we use the hat notation for the helicities in the W -decay system. We evaluate the helicity amplitudes in the $(\ell^- \bar{\nu}_\ell)$ center-of-mass (CM) system, with ℓ^- defining the z -direction such that $\hat{\lambda}_W = \lambda_\ell - 1/2$. The label (J) takes the values $(J = 0)$ with $\lambda_W = 0$ ($:= t$) and $(J = 1)$ with $\lambda_W = \pm 1, 0$ for the lepton current J_W^μ , respectively. The relevant spinors are given by [56]

$$\bar{u}_2(\pm \frac{1}{2}, p_\ell) = \sqrt{E_\ell + m_\ell} \left(\chi_\pm^\dagger, \frac{\mp |\mathbf{p}_\ell|}{E_\ell + m_\ell} \chi_\pm^\dagger \right), \quad v_{\bar{\nu}}(\frac{1}{2}, p_{\bar{\nu}_\ell}) = \sqrt{E_\nu} \begin{pmatrix} \chi_+ \\ -\chi_+ \end{pmatrix}, \quad (\text{B2})$$

where $\chi_+ = \begin{pmatrix} 1 \\ 0 \end{pmatrix}$ and $\chi_- = \begin{pmatrix} 0 \\ 1 \end{pmatrix}$ are the usual Pauli two-spinors. The lepton-side helicity amplitudes can be calculated to be

$$\begin{aligned} h_{t; +1/2 +1/2}(J = 0) &= 2\sqrt{v} m_\ell, \\ h_{0; +1/2 +1/2}(J = 1) &= 2\sqrt{v} m_\ell, \\ h_{-1; -1/2 +1/2}(J = 1) &= 2\sqrt{2} \sqrt{q^2} \sqrt{v}, \end{aligned} \quad (\text{B3})$$

where, as before, $v = 1 - m_\ell^2/q^2$ is the lepton velocity in the $(\ell^- \bar{\nu}_\ell)$ CM frame. On squaring the lepton-side $V - A$ helicity amplitudes one finds

$$\begin{aligned} |h_{t; +1/2 +1/2}|^2 &= |h_{0; +1/2 +1/2}|^2 = 4m_\ell^2 v = 8q^2 v \delta_\ell, \\ h_{t; +1/2 +1/2} h_{0; +1/2 +1/2} &= 4m_\ell^2 v = 8q^2 v \delta_\ell, \\ |h_{-1; -1/2 +1/2}|^2 &= 8q^2 v. \end{aligned}$$

The helicity flip contributions can be seen to be suppressed relative to the helicity nonflip contributions by the factor $\delta_\ell = m_\ell^2/2q^2$, i.e. $|h_{hf}|^2/|h_{nf}|^2 = \delta_\ell$.

One can go through the same exercise for $W_{\text{off-shell}}^+ \rightarrow \ell^+ \nu_\ell$ with the z -direction defined by ℓ^+ , i.e. ($\hat{\lambda}_W = \lambda_\ell + 1/2$). The helicity amplitudes are defined by

$$h_{\hat{\lambda}_W; \lambda_{\ell^+}, -1/2}(J) = \bar{u}_{\nu_\ell}(-1/2) \gamma_\mu (1 - \gamma_5) v_{\ell^+}(\lambda_{\ell^+}) \epsilon^\mu(\hat{\lambda}_W), \quad (\text{B4})$$

which can be evaluated with the explicit forms of the spinors

$$\bar{u}_{\nu_\ell}(-\frac{1}{2}, p_{\nu_\ell}) = -\sqrt{E_\nu} \left(\chi_+^\dagger, \chi_+^\dagger \right) \quad v_{\ell^+}(\pm \frac{1}{2}, p_\ell) = \sqrt{E_\ell + m_\ell} \begin{pmatrix} \frac{-|\mathbf{p}_\ell|}{E_\ell + m_\ell} \chi_\mp \\ \pm \chi_\mp \end{pmatrix}, \quad (\text{B5})$$

and one finds

$$\begin{aligned} h_{t; -1/2 -1/2}(J = 0) &= -2\sqrt{v} m_\ell, \\ h_{0; -1/2 -1/2}(J = 1) &= -2\sqrt{v} m_\ell, \\ h_{+1; +1/2 -1/2}(J = 1) &= -2\sqrt{2} \sqrt{q^2} \sqrt{v}. \end{aligned} \quad (\text{B6})$$

The lepton tensor helicity components for the two cases are given by (we assume the lepton-side helicity amplitudes to be relatively real)

$$\begin{aligned}
\text{unpolarized case:} \quad & \hat{L}_{\hat{\lambda}_W \hat{\lambda}'_W} = \sum_{\lambda_\ell} h_{\hat{\lambda}_W; \lambda_\ell \pm 1/2} h_{\hat{\lambda}'_W; \lambda_\ell \pm 1/2} \\
\text{longitudinal polarization:} \quad & \hat{L}_{\hat{\lambda}_W \hat{\lambda}'_W}(s_z) = |h_{\hat{\lambda}_W; 1/2 \pm 1/2}|^2 - |h_{\hat{\lambda}'_W; -1/2 \pm 1/2}|^2 \\
\text{transverse polarization:} \quad & \hat{L}_{\hat{\lambda}_W \hat{\lambda}'_W}(s_x) = 2 h_{\hat{\lambda}_W; 1/2 \pm 1/2} h_{\hat{\lambda}'_W; -1/2 \pm 1/2}
\end{aligned} \tag{B7}$$

Inserting the lepton-side helicity amplitudes, one reproduces the results of Eqs. (A9), (A14) and (A19).

-
- [1] A. Soffer, *Mod. Phys. Lett. A* **29**, 1430007 (2014) [arXiv:1401.7947 [hep-ex]].
- [2] A. Celis, arXiv:1410.1858 [hep-ph].
- [3] A. Crivellin, arXiv:1409.0922 [hep-ph].
- [4] T. Blake, T. Gershon and G. Hiller, arXiv:1501.03309 [hep-ex].
- [5] J. P. Lees *et al.* [BaBar Collaboration], *Phys. Rev. Lett.* **109**, 101802 (2012) [arXiv:1205.5442 [hep-ex]].
- [6] A. Matyja *et al.* [Belle Collaboration], *Phys. Rev. Lett.* **99**, 191807 (2007) [arXiv:0706.4429 [hep-ex]].
- [7] A. Bozek *et al.* [Belle Collaboration], *Phys. Rev. D* **82**, 072005 (2010) [arXiv:1005.2302 [hep-ex]].
- [8] Y. Sakaki, M. Tanaka, A. Tayduganov and R. Watanabe, arXiv:1412.3761 [hep-ph].
- [9] U. Nierste, S. Trine and S. Westhoff, *Phys. Rev. D* **78**, 015006 (2008) [arXiv:0801.4938 [hep-ph]].
- [10] A. Pich and P. Tuzon, *Phys. Rev. D* **80**, 091702 (2009) [arXiv:0908.1554 [hep-ph]].
- [11] M. Jung, A. Pich and P. Tuzon, *JHEP* **1011**, 003 (2010) [arXiv:1006.0470 [hep-ph]].
- [12] S. Faller, T. Mannel and S. Turczyk, *Phys. Rev. D* **84**, 014022 (2011) [arXiv:1105.3679 [hep-ph]].
- [13] A. Celis, M. Jung, X. Q. Li and A. Pich, *JHEP* **1301**, 054 (2013) [arXiv:1210.8443 [hep-ph]].
- [14] S. Fajfer, J. F. Kamenik, I. Nisandzic and J. Zupan, *Phys. Rev. Lett.* **109**, 161801 (2012) [arXiv:1206.1872 [hep-ph]].
- [15] S. Fajfer, J. F. Kamenik and I. Nisandzic, *Phys. Rev. D* **85**, 094025 (2012) [arXiv:1203.2654 [hep-ph]].
- [16] A. Datta, M. Duraisamy and D. Ghosh, *Phys. Rev. D* **86**, 034027 (2012) [arXiv:1206.3760 [hep-ph]].
- [17] A. Crivellin, C. Greub and A. Kokulu, *Phys. Rev. D* **86**, 054014 (2012) [arXiv:1206.2634 [hep-ph]].
- [18] X. G. He and G. Valencia, *Phys. Rev. D* **87**, 014014 (2013) [arXiv:1211.0348 [hep-ph]].
- [19] M. Tanaka and R. Watanabe, *Phys. Rev. D* **87**, 034028 (2013) [arXiv:1212.1878 [hep-ph]].
- [20] P. Biancofiore, P. Colangelo and F. De Fazio, *Phys. Rev. D* **87**, 074010 (2013) [arXiv:1302.1042 [hep-ph]].
- [21] M. Duraisamy, P. Sharma and A. Datta, *Phys. Rev. D* **90**, 074013 (2014) [arXiv:1405.3719 [hep-ph]].
- [22] J. G. Körner and G. A. Schuler, *Z. Phys. C* **38**, 511 (1988) [Erratum-ibid. C **41**, 690 (1989)].
- [23] J. G. Körner and G. A. Schuler, *Phys. Lett. B* **231**, 306 (1989).
- [24] J. G. Körner and G. A. Schuler, *Z. Phys. C* **46**, 93 (1990).
- [25] T. Gutsche, M. A. Ivanov, J. G. Körner, V. E. Lyubovitskij and P. Santorelli, *Phys. Rev. D* **87**, 074031 (2013) [arXiv:1301.3737 [hep-ph]].
- [26] T. Gutsche, M. A. Ivanov, J. G. Körner, V. E. Lyubovitskij and P. Santorelli, *Phys. Rev. D* **88**, 114018 (2013) [arXiv:1309.7879 [hep-ph]].
- [27] T. Gutsche, M. A. Ivanov, J. G. Körner, V. E. Lyubovitskij and P. Santorelli, *Phys. Rev. D* **90**, 114033 (2014) [arXiv:1410.6043 [hep-ph]].
- [28] J. G. Körner, M. Krämer and D. Pirjol, *Prog. Part. Nucl. Phys.* **33**, 787 (1994) [hep-ph/9406359].
- [29] J. G. Körner and M. Krämer, *Phys. Lett. B* **275**, 495 (1992).
- [30] F. Krüger and J. Matias, *Phys. Rev. D* **71**, 094009 (2005).
- [31] G. Buchalla, O. Cata and G. D'Ambrosio, *Eur. Phys. J. C* **74**, 2798 (2014) [arXiv:1310.2574 [hep-ph]].
- [32] S. R. Gevorkyan and M. H. Misheva, *Eur. Phys. J. C* **74**, 2860 (2014) [arXiv:1403.1053 [hep-ph]].
- [33] A. Kadeer, J. G. Körner, U. Moosbrugger, *Eur. Phys. J.* **C59**, 27 (2009) [hep-ph/0511019].
- [34] M. E. Rose, *Elementary Theory of Angular Momentum*, (Wiley, New York, 1957)
- [35] P. Bialas, J. G. Körner, M. Krämer, K. Zalewski, *Z. Phys.* **C57**, 115 (1993).
- [36] M. Fischer, S. Groote, J. G. Körner and M. C. Mauser, *Phys. Rev. D* **70**, 094026 (2004) [hep-ph/0309047].
- [37] M. Fischer, S. Groote, J. G. Körner, M. C. Mauser and B. Lampe, *Phys. Lett. B* **451**, 406 (1999) [hep-ph/9811482].
- [38] M. Fischer, S. Groote, J. G. Körner and M. C. Mauser, *Phys. Rev. D* **65**, 054036 (2002) [hep-ph/0101322].
- [39] K. A. Olive *et al.* [Particle Data Group Collaboration], *Chin. Phys. C* **38**, 090001 (2014).
- [40] J. G. Körner and M. Krämer, *Z. Phys. C* **55**, 659 (1992).
- [41] B. König, J. G. Körner and M. Krämer, *Phys. Rev. D* **49**, 2363 (1994) [hep-ph/9310263].
- [42] T. Gutsche, M. A. Ivanov, J. G. Körner, V. E. Lyubovitskij and P. Santorelli, *Phys. Rev. D* **86**, 074013 (2012) [arXiv:1207.7052 [hep-ph]].
- [43] J. Abdallah *et al.* (DELPHI Collaboration), *Phys. Lett. B* **585**, 63 (2004) [hep-ex/0403040].
- [44] B. König, J. G. Körner, M. Krämer and P. Kroll, *Phys. Rev. D* **56**, 4282 (1997) [hep-ph/9701212].
- [45] M. A. Ivanov, V. E. Lyubovitskij, J. G. Körner and P. Kroll, *Phys. Rev. D* **56**, 348 (1997) [hep-ph/9612463].

- [46] J. G. Körner and B. Melic, Phys. Rev. D **62**, 074008 (2000) [hep-ph/0005141].
 [47] M. Q. Huang, H. Y. Jin, J. G. Körner and C. Liu, Phys. Lett. B **629**, 27 (2005) [hep-ph/0502004].
 [48] M. Pervin, W. Roberts and S. Capstick, Phys. Rev. C **72**, 035201 (2005) [nucl-th/0503030].
 [49] D. Ebert, R. N. Faustov and V. O. Galkin, Phys. Rev. D **73**, 094002 (2006) [hep-ph/0604017].
 [50] H. W. Ke, X. Q. Li and Z. T. Wei, Phys. Rev. D **77**, 014020 (2008) [arXiv:0710.1927 [hep-ph]].
 [51] A. G. Grozin and O. I. Yakovlev, Phys. Lett. B **291**, 441 (1992).
 [52] R. M. Woloshyn, PoS Hadron **2013**, 203 (2013).
 [53] F. Hussain, J. G. Körner, M. Krämer and G. Thompson, Z. Phys. C **51**, 321 (1991).
 [54] Y. Amhis *et al.* [Heavy Flavor Averaging Group (HFAG) Collaboration], arXiv:1412.7515 [hep-ex].
 [55] A. Zupanc *et al.* [Belle Collaboration], Phys. Rev. Lett. **113**, 042002 (2014) [arXiv:1312.7826 [hep-ex]].
 [56] P.R. Auvil and J.J. Brehm, Phys. Rev. **145**, 1152 (1966).

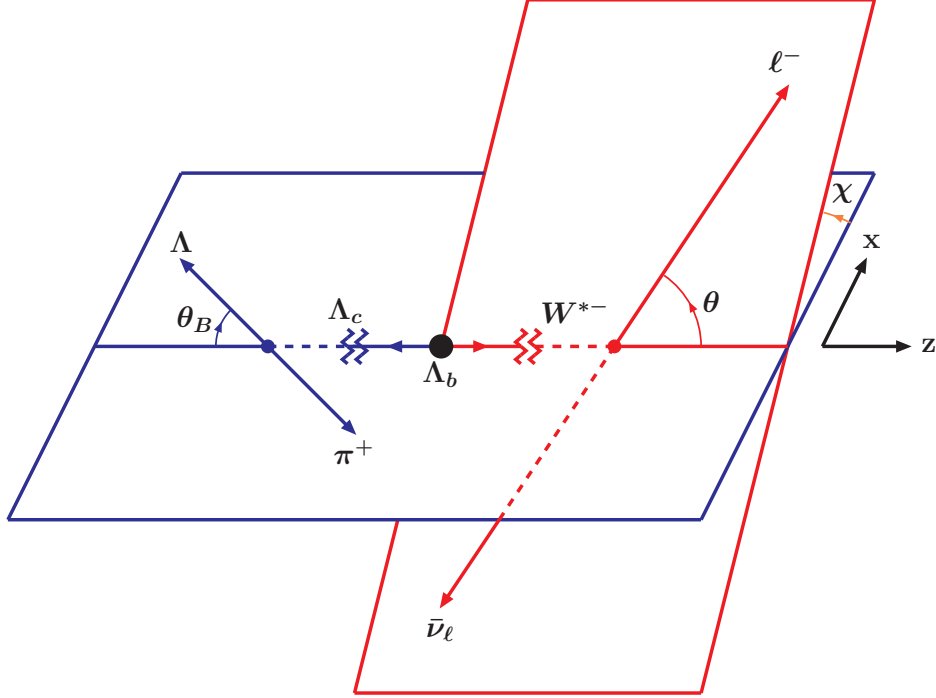


FIG. 1: Definition of the polar angles θ , θ_B and the azimuthal angle χ .

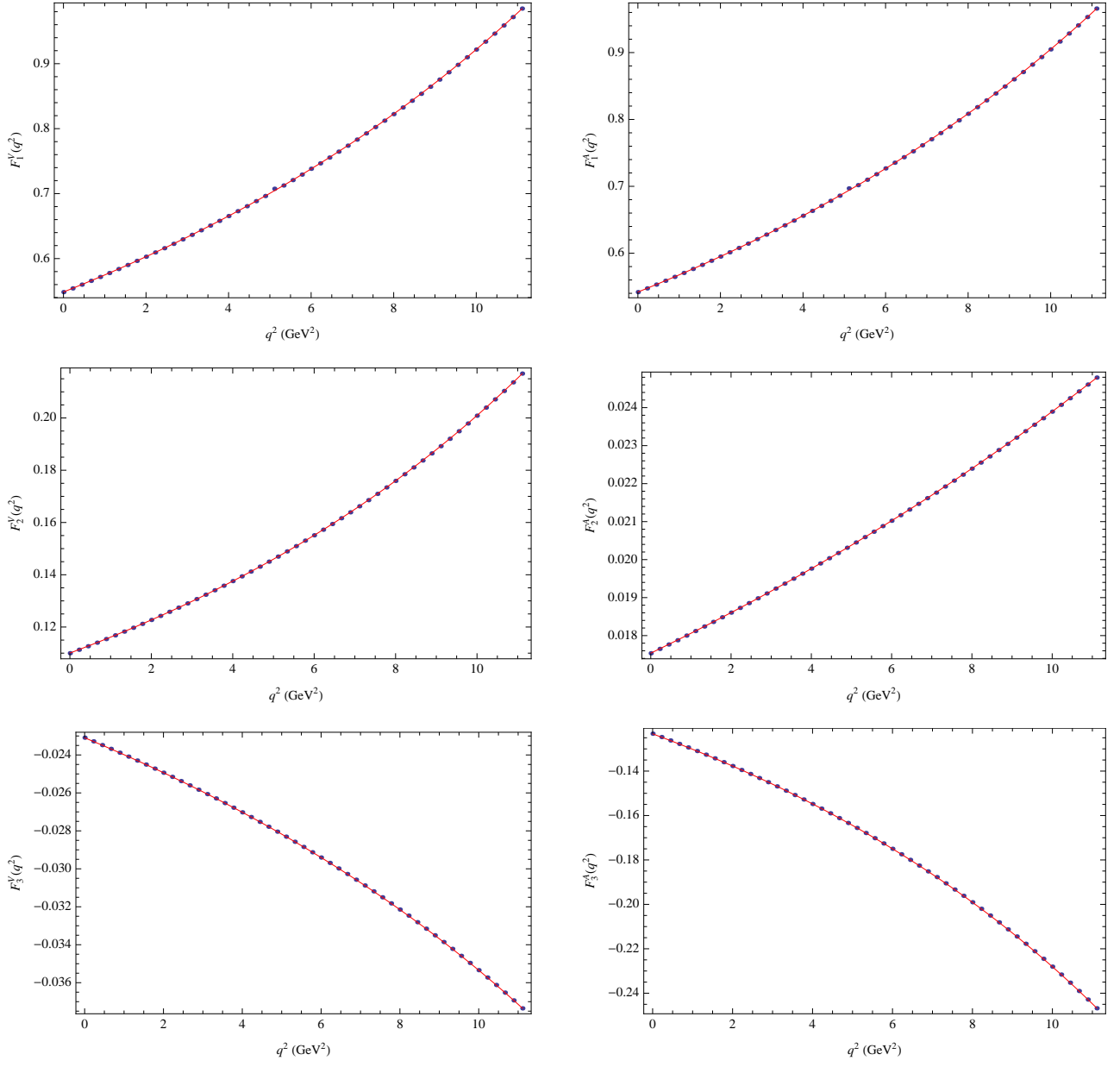


FIG. 2: Form factors defining the transition $\Lambda_b \rightarrow \Lambda_c$: approximated results (solid line), exact result(dotted line).

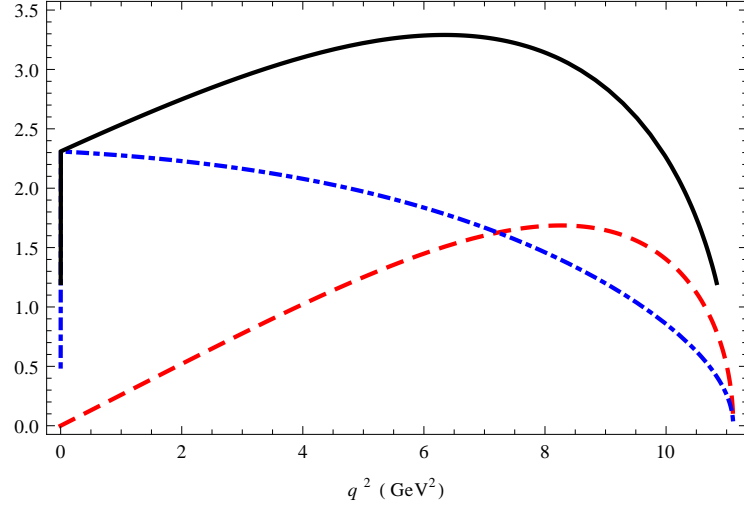


FIG. 3: The q^2 -dependence of the partial rates $d\Gamma_U/dq^2$ (dashed), $d\Gamma_L/dq^2$ (dot-dashed) and their sum $d\Gamma_{U+L}/dq^2$ (solid) for the e^- -mode (in units of $10^{-15} \text{ GeV}^{-1}$).

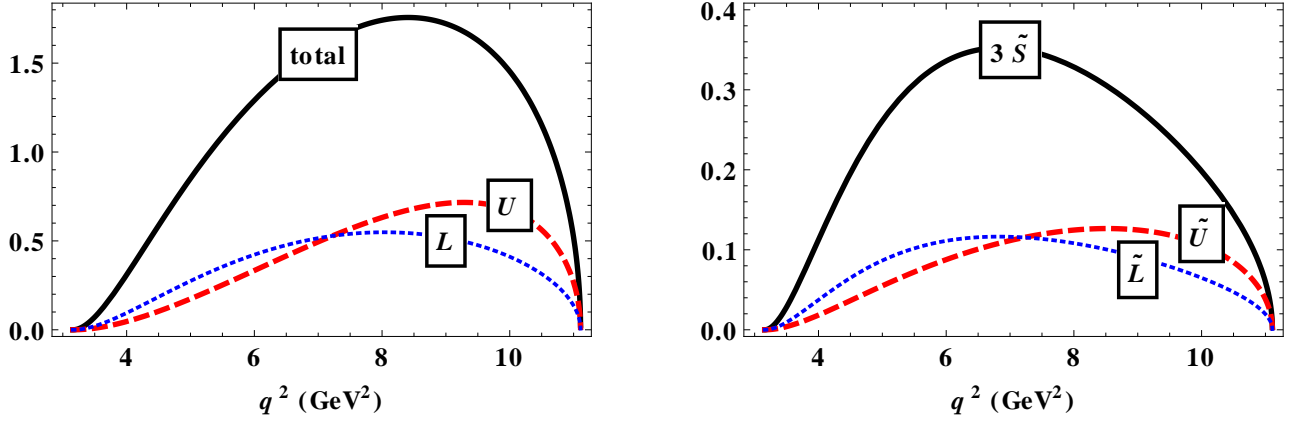


FIG. 4: The q^2 -dependence of the partial nonflip rates $d\Gamma_{U,L}/dq^2$, and the flip rates $d\tilde{\Gamma}_{U,L}/dq^2$ and $3d\tilde{\Gamma}_S/dq^2$ for the τ^- -mode (in units of $10^{-15} \text{ GeV}^{-1}$). Also shown is the total rate $d\Gamma_{U+L}/dq^2 + d\tilde{\Gamma}_{U+L}/dq^2 + 3d\tilde{\Gamma}_S/dq^2$.

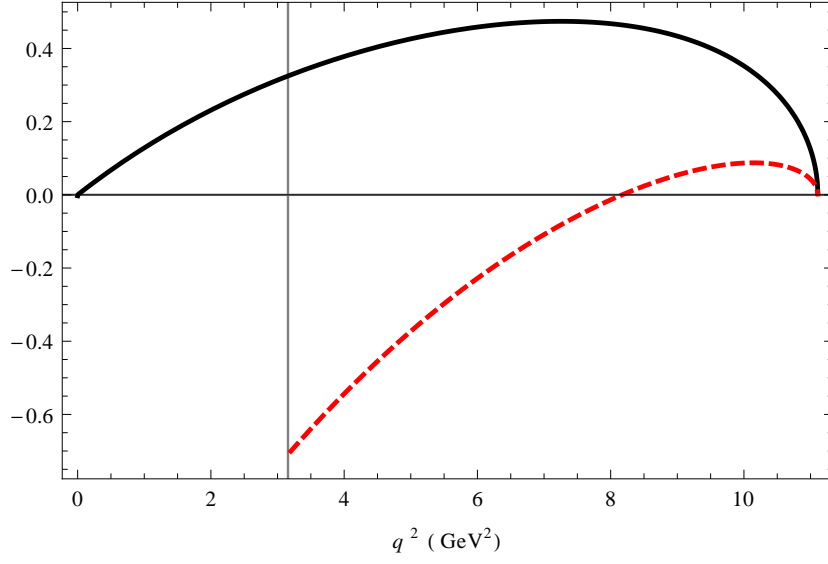


FIG. 5: The q^2 -dependence of the lepton-side forward-backward asymmetry $A_{FB}^{\ell}(q^2)$ for the e^- - (solid) and τ^- -mode (dashed).

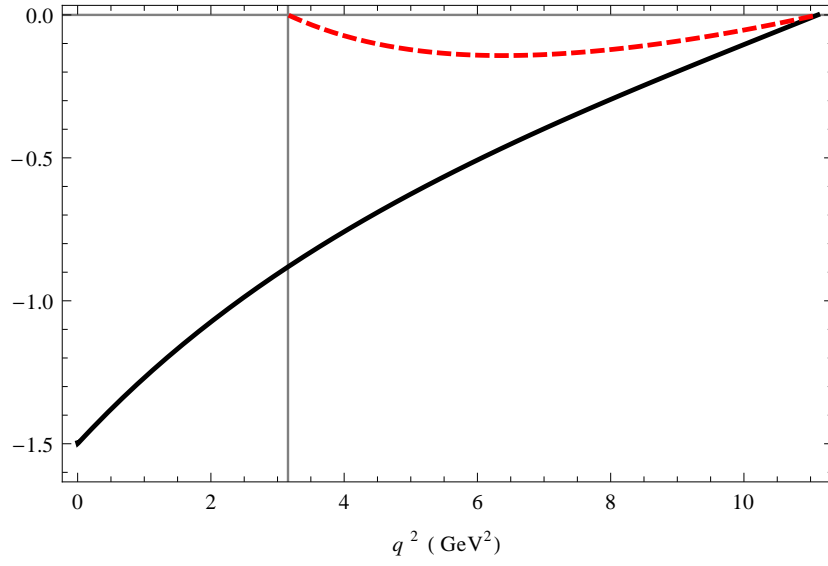


FIG. 6: The q^2 -dependence of the convexity parameter $C_F(q^2)$ for the e^- - (solid) and τ^- -mode (dashed).

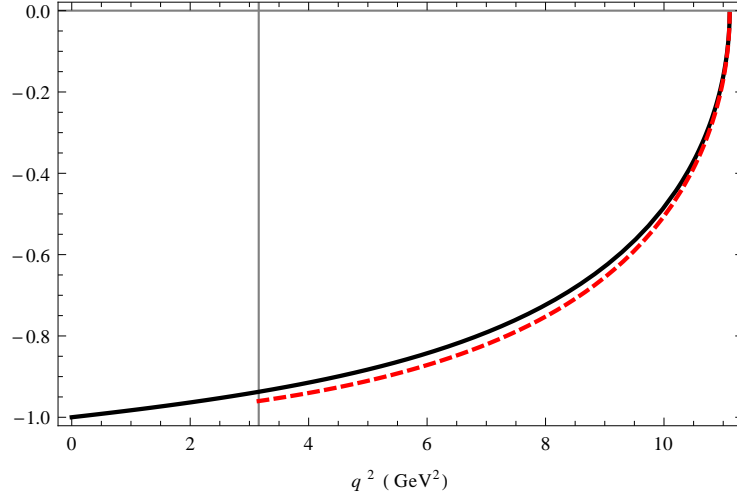


FIG. 7: The q^2 -dependence of the longitudinal polarization component $P_z^h(q^2)$ of the daughter baryon Λ_c for the e^- - (solid) and τ^- -mode (dashed).

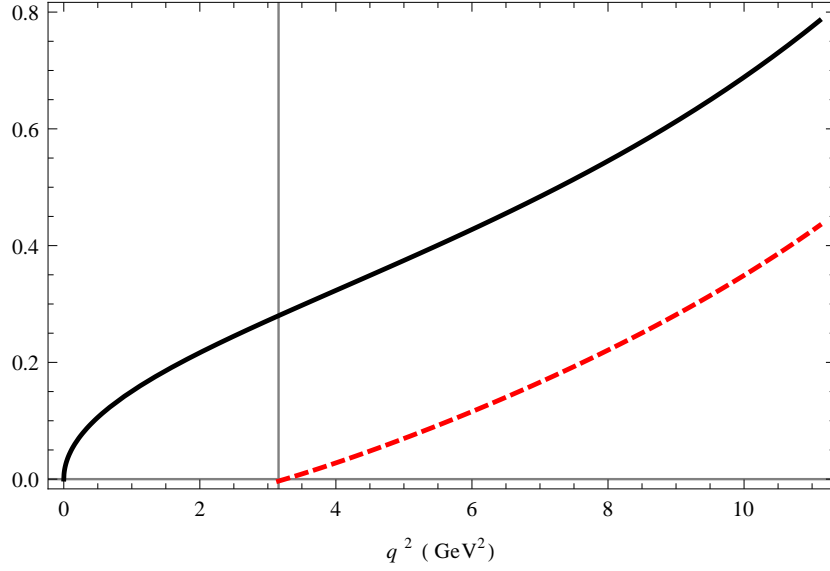


FIG. 8: The q^2 -dependence of the transverse polarization component $P_x^h(q^2)$ of the daughter baryon Λ_c for the e^- - (solid) and τ^- -mode (dashed).

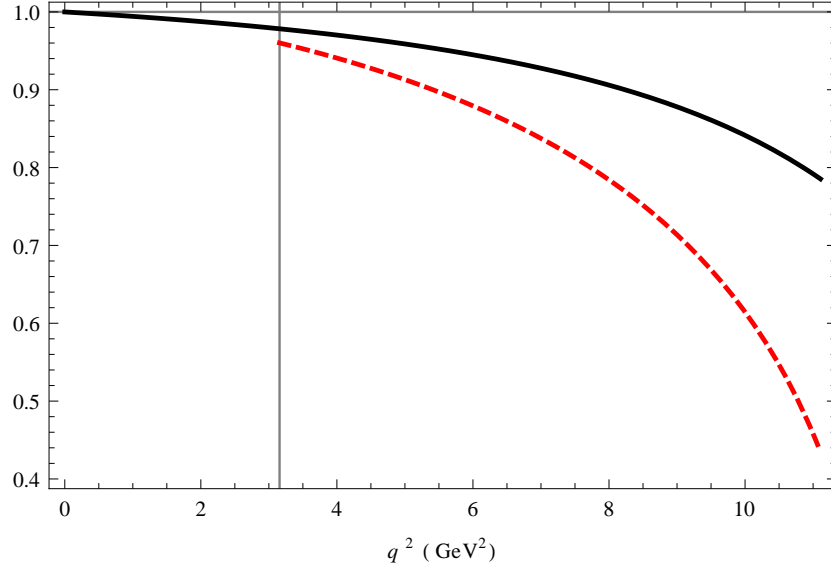


FIG. 9: The q^2 -dependence of the total Λ_c polarization $|\vec{P}^h|(q^2) = \sqrt{(P_x^h)^2 + (P_z^h)^2}$ for the e^- - (solid) and τ^- -mode (dashed).

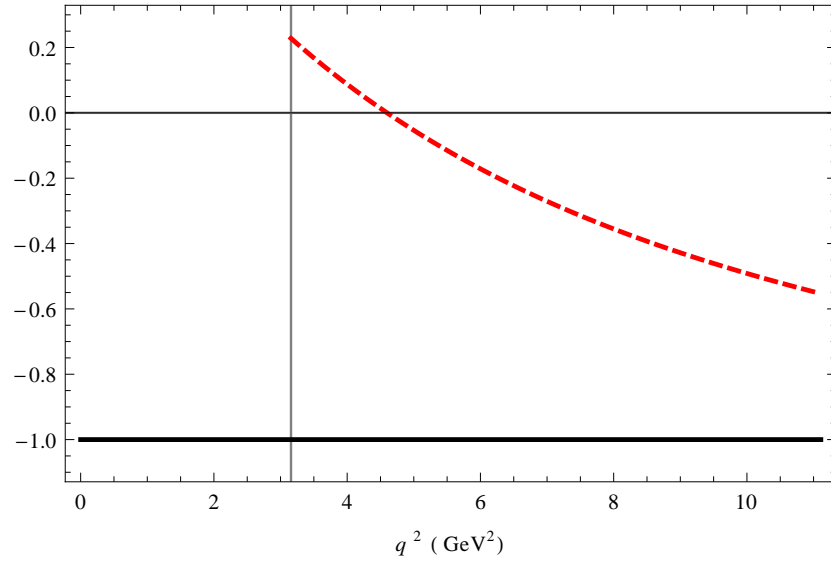


FIG. 10: The q^2 -dependence of the longitudinal polarization component $P_z^\ell(q^2)$ for the charged leptons e^- - (solid) and τ^- -mode (dashed).

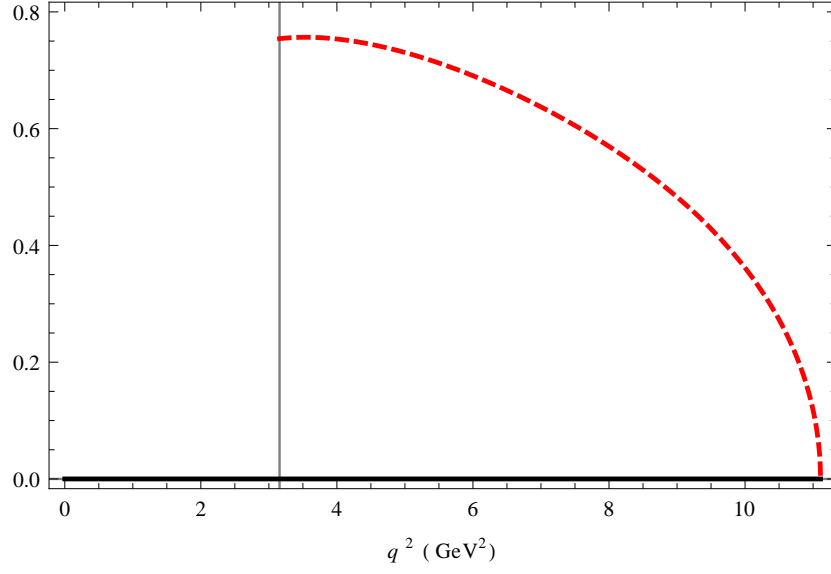


FIG. 11: The q^2 -dependence of the transverse polarization component $P_x^\ell(q^2)$ for the charged leptons e^- (solid) and τ^- -mode (dashed).

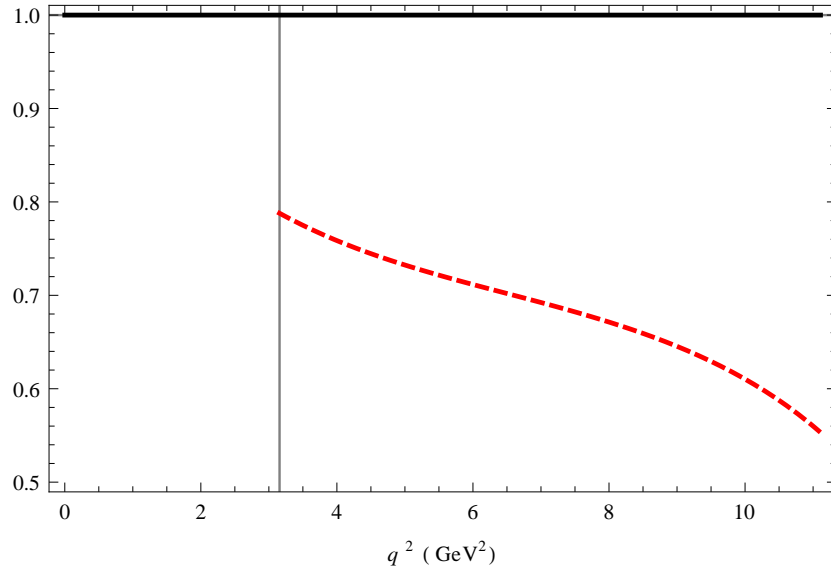


FIG. 12: The q^2 -dependence of the total lepton polarization $|\vec{P}^\ell|(q^2) = \sqrt{(P_x^\ell)^2 + (P_z^\ell)^2}$ for the e^- (solid) and τ^- -mode (dashed).